MECHANICAL PROPERTIES OF Mn - Si - V DUAL PHASE STEELS

A Thesis Submitted
In Partial Fulfilment of the Requirements
for the Degree of
MASTER OF TECHNOLOGY

by

VIKAS KUMAR

to the
DEPARTMENT OF METALLURGICAL ENGINEERING
INDIAN INSTITUTE OF TECHNOLOGY, KANPUR
AUGUST, 1982

To

My Mother

ME-1982-M-KUM-MEC

CERTIFICATE

This is to certify that the thesis entitled

"MECHANICAL PROPERTIES OF Mn-Si-V DUAL PHASE STEELS" by

Mr. Vikas Kumar is the record of work carried out under

our supervision and has not been submitted elsewhere for

a degree.

(R. K. RAY)
Assistant Professor
Department of Metallurgical
        Engineering
Indian Institute of Technology
Kanpur

(Abroad on long leave)

August 1982.

(G. S. MURTY)
Head and Professor
Department of Metallurgical
        Engineering
Indian Institute of Technology
Kanpur

iii

ACKNOWLEDGEMENTS

I take this opportunity to express my deep and profound sense of gratitude to Dr. R.K. Ray and Dr. G.S. Murty for their valuable guidance and critical appraisal throughout the work.

Thanks are due to all my friends for making my stay at I.I.T. Kanpur a pleasant and memorable experience.

Special thanks are due to Mr. V.P. Gupta for tracing the figures and Mr. R.N. Srivastava for typing.

Vikas Kumar

CONTENTS

LIST OF TABLES

LIST OF FIGURES

ABSTRACT

Newly developed dual phase steels possess good formability and high strength. These exhibit a low yield to tensile strength ratio, high initial work hardening rate and large elongations in comparison to HSLA steels. These unique properties arise from the microstructural features of dispersed islands of martensite in ferrite matrix.

In this study the interrelation between the mechanical response and microstructural features of dual phase Mn-Si-V steels of four compositions have been explored. For this purpose, these steels were quenched from austenite plus ferrite phase field choosing different parameters such as initial austenitizing temperature, intercritical annealing temperature and alloy content. The tensile properties, toughness and Bauschinger behavior were evaluated from mechanical tests. The microstructural aspects of the alloys were studied by optical microscopy. The heat treatments at higher intercritical temperature coupled with lower austenitizing temperature yielded higher strength, toughness and Bauschinger effect. Further, there was improvement in strength by addition of silicon and manganese. The magnitude of Bauschinger effect and toughness increased with manganese content but adversely affected by silicon content.

CHAPTER I

INTRODUCTION

Reduction in the weight of an automobile is highly
beneficial in minimising the fuel consumption. A direct approach
to automobile weight reduction is vehicle size reduction. Further
weight reduction may be attained by material substitution with
plastic, aluminium or higher strength steels as replacement for
plain carbon steels. Unlike plastics and aluminium, high
strength steels have the same density as plain carbon steels but
weight can be reduced by using thinner section to carry out the
same load. Substitution with the high strength steels would
usually require less modification of existing manufacturing
processes and equipment than substitution with plastic or
aluminium.

These high strength steels, such as SAE 950X or SAE
980X, high strength low alloy steels; have the same composition
as plain carbon steels with minor additions of V, Nb or Ti.
They are thermomechanically processed and are considerably
stronger, but are less formable than plain carbon steels. This
has limited the widespread use of these steels in automobile
applications.

Dual-phase steels belong to a newly developed class of
high strength low alloy (HSLA) steels in which the microstructure
consists of 80-85% of a matrix of ferrite, with dispersed islands
of a second phase (martensite). These steels are produced either

by direct hot rolling or by continuous annealing or bath
annealing of hot or cold rolled steels. They possess good
formability and high strength in the formed component and thus
satisfy the requirements of components of automobile industry.

The dual phase steels are characterized by a low ratio
of yield to tensile strength (0.5-0.6), high initial work
hardening rate and total elongation of 30% as compared with
18-20% for a microalloyed steel with the same tensile strength.
Further, there is no yield point elongation i.e. no disconti-
nuous yielding, in dual phase steels. A number of potential
uses for dual phase steels have been envisaged in various load
bearing and stamped automobile components such as bumpers,
bumper reinforcements, jack posts, wheel rims, wheel hood, deck
lid, discs, door inner panels and tail gate outer panels. An
estimate shows that dual phase steels can be used to the extent
of 250 Kgs on a medium sized car, giving rise to a weight saving
of about 80 Kgs.

The objective of the present work is to critically
study the parameters controlling the structure and the mechanical
properties of a few dual phase steels. An attempt has also been
made to assess as to how these parameters influence the
Bauschinger effect in dual phase steels of different compositions.

CHAPTER II

LITERATURE REVIEW

The three successive conferences in recent years on the development, production, processing, properties and economics of dual phase steels at Chicago (1977)[1], Berlin (1978)[2] and New Orleans (1979)[3] are the indications of the importance attached to the development of dual phase steels.

In the present review the various factors controlling the microstructure and properties in dual phase steels are critically surveyed on the basis of available literature. Various simple models used to describe the plastic deformation in dual phase steels are also discussed.

2.1 Historical Developments:

Davies and Wilshire[4] were among the first to produce the dual phase microstructure by intercritical annealing. Shortly afterwards Cairne and Charles[5] recognized the improvement in properties of a composite structure of soft ferrite and fibrous martensite. Grange[6] noted a few years later that steels quenched from the intercritical region have a low yield to tensile strength ratio and an improved elongation. Similar dual phase properties were obtained in manganese steels by Matsuoka and Yamamori[7] who found that these steels had a high work hardening rate, good press formability and spot weldability. Hayami and Furukawa[8] developed Mn-Si dual phase steels with low yield strength and continuous yielding. At about the same time,

Rashid[9,10] developed a heat treatment schedule for annealing a
vanadium microalloyed steel (VAN80) to produce the dual phase
structure and properties. Koo and Thomas[11,12] utilized the
grain refinement technique of cyclic austenitization and
produced dual phase properties in Mn, Si and Cr steels.
Davies[13-17] made detailed investigations on manganese steels and
interpreted the variations in strength and ductility in terms
of Mileiko's theory[18] for composites of two ductile phases.
Speich and Miller[19] considered the ternary phase relationships
of Fe, Mn and C and related strength and ductility of dual phase
steels both to the volume fraction of second phase (martensite)
and its carbon content using the composite theory of Tamura et
al.[20] Bucher and Hamburg[21] extended the formability studies[10]
of Rashid on VAN80 steels and also obtained a range of strength-
ductility combinations. Following the work of Hayami and
Furukawa[8], other Japanese workers[22-25] studied in detail the
effect of cooling rate and showed that mild cooling rates tended
to produce a clean ferrite and are suitable for production in
the as-rolled condition. The Climax group of workers[26-28]
produced dual phase properties mainly in steels containing
molybdenum. Similar steels were studied by other workers.[29,30]
Marder and Rigsbee et al.[31,32] emphasized the role of retained
austenite on high work hardening rate observed in dual phase
steels. Full scale plant production of dual phase steels has
also been attempted.[33,34] Today these steels are available
under a number of trade names such as GM980X, VAN-QN, Hiform
80D, dual phase 80, Nippon 60 and Nippon 100.

2.2 Production Routes:

Various routes have been adopted for the commercial production of dual phase steels.[21,24,32] Depending upon chemical composition, economics, the following process have been developed

(i) Production of dual phase steels in the as-hot-rolled condition (the AHR Process). It has also been called the as-rolled dual phase (ARDP) steel.

(ii) Continuous annealing (CA) of either hot-rolled or cold rolled sheets.

(iii) Batch annealing (BA) is the process where hot rolled or cold rolled coiled sheets or cut sheets are annealed in batches.

The as hot-rolled process requires no special extra equipment over the conventional hot mill, except for the provision of facilities for the control of speed and rate of cooling on the run-out table. Special combinations of alloying elements added to control hardenability need to be more selective in their effects, causing differential retardation of polygonal ferrite, pearlite and bainite transformations. The C.C.T diagrams for Mn-Si-Cr-Mo steels have been developed by Coldren et al.[35]

Furukawa et al.[24] have tried the production of as-hot-rolled dual phase structure from a simple C-Mn-Si aluminium killed steel, with the composition: 0.09 C-1.5 Mn-0.5 Si. The process consists of a low finishing rolling temperature in the intercritical region and cooling at a rate of 40°C/sec followed

by cooling in the range of 100°C which is below Ms.

In continuous annealing process[36] , hot rolled or cold rolled sheets are uncoiled and passed through a continuous annealing furnace, the temperature of which is maintained in the intercritical region or above A_3. After annealing, a controlled cooling rate is adopted depending upon the chemistry of the steel. Special equipment and additional heat treatment step are involved as compared to as-hot-rolled process.

In batch annealing[32], tight or open coils are heated to an intercritical annealing temperature either in a stationary or a continuous furnace. After heating,the coils are cooled in air or quenched into water depending upon the chemistry of the steel.

2.3 Structure-Property Relationships:

It is well documented that the mechanical properties of dual phase steels are affected by volume fraction of martensite, the individual properties of ferrite and martensite and morphology of ferrite and martensite.

A study has been made of the effect of volume fraction of martensite on strength of Mn dual phase steels.[13,14] It was observed that there is a linear increase in yield and tensile strengths with the volume fraction of second phase in a number of manganese dual phase steels given different heat treatments. It appears that the strength is governed by the rule of mixture between a strong martensite and week ferrite phase

Further, in a study[22] it is found that the product of UTS and elongation, which may be taken as a measure of the good combination of properties, remains approximately constant upto about 20% martensite and thereafter declines with increasing martensite content. Thus the optimum properties are attained at about 20% martensite. The reason given to the change at 20% martensite is that above that level the large martensite content accelerates void formation strongly such that the fibrous fracture supersedes necking and thereby impairs the total ductility.

The strength of martensite is a function of its carbon content. With increasing carbon, the martensite becomes stronger, until a stage is reached when martensite substructure changes from parallel laths to non-parallel internally-twinned plates which are brittle. In a study of substructure of martensite in dual phase steels, it was suggested that lath martensite forming at lower carbon contents of about 0.3-0.4% is desirable in dual phase steels because it has a high strength but not brittle.[37]

The distribution of the second phase (martensite) is also important in determining the dual phase properties. Becker and Hornbogen[38] have analysed the distribution in two phase mixtures in terms of the parameters which is defined as:

$$\Delta = \frac{C_{ss}}{C_{\alpha\alpha}}$$

where C_{ss} is the density of second phase/second phase grain boundaries and $C_{\alpha\alpha}$ is the density of ferrite/ferrite grain

boundaries when $\triangle = \infty$, $C_{\alpha\alpha}$ tends to zero and a network structure is obtained where each grain of ferrite is outlined by a continuous film of martensite. If $\triangle = 0$, the martensite is dispersed as isolated islands in ferrite matrix. In the dual phase steel, where martensite volume fraction is between 0.15-0.20, the distribution lies between these two extreme types. The nature and distribution of the two phases in the micro-structure are determined by nucleation conditions for the formation of various phases during heating and cooling.

Ostrom and Lindgren[39] found that after annealing in the intercritical region, the martensite occurs as chains of islands along ferrite grain boundaries whereas after annealing above A_3, the martensite grains are more isolated. Koo and Thomas[12,40] found that the presence of chromium in the steel increases the connectivity of martensite. An extensively connected martensite tends to reduce the total elongation and reduction in area.[37] The strength of the steel, however, tends to be less sensitive than the ductility to the martensitic distribution.[37]

In a recent study[41] on the effects of morphology of martensite on the mechanical behavior of dual phase steels, it is concluded that

(i) The structure containing coarse martensite surrounded by ferrite has much lower ductility than the structure containing fine fibrous and fine globular martensite in ferrite matrix.

(ii) The failure of coarse martensitic dual phase structure is due to the initiation of cleavage cracks in ferrite

matrix, while in the fine fibrous and fine globular martensitic structures, failure occurs by void nucleation and coalescence.

(iii)   In all types of martensite morphologies studied, crack propagates primarily in the ferrite matrix rather than into the martensite.

Retained austenite has been identified in three different forms in dual phase steels in amounts varying from 1% to 8%. It occurs as thin layers interspersed between lath of martensite.[42] This amount is usually < 1% and requires careful selected area diffraction in an electron microscope for identification. Retained austenite occurs as a part of the second phase (martensite), in a more coarse form and can be identified by X-ray methods.[31-33] This comprises the major part of the various forms of retained austenite. Fine island like isolated particles of retained austenite (~1 micron size) may also occur at grain corners and within ferrite grains. Some workers believe that retained austenite transforms to martensite during straining of these steels and it may increase the work hardening rate to such an extent that UTS is improved.

The mechanical properties of ferrite matrix control the ductility of dual phase steels but influence the strength of these steels to a lesser extent.[43] The features of the ferrite matrix that affect the properties of dual phase steels are:

   (i)   morphology of ferrite,

  (ii)   the ferrite grain size

(iii)   the presence of precipitates in the matrix, and

 (iv)   the interstitial and substitutional solutes in it.

The ferrite grains must be equiaxed (polygonal) in shape since this gives good and uniform properties. Accicular ferrite that forms at lower transformation temperatures in some compositions impairs the ductility even though the strength usually increases.

On the basis of the fact that uniform elongation remains constant with decreasing grain size in pure ferrite, a fine ferrite grain size is considered to be favourable for the combination of UTS and elongation in dual phase steels.

The presence of carbide or carbonitride precipitates, especially in a fine distributed form, is not considered desirable in ferrite matrix since it lowers ductility.[30,37] The composition and heat treatment of dual phase steels should be controlled in such a way that fine carbide precipitates do not form, particularly at grain boundaries[10]. It is often stated in literature that the ferrite in dual phase steels should be clean, that it should be as free as possible of interstitials and precipitates. This is usually the motivation why mild cooling rates should be preferred to quenching after the anneal. However, slow cooling rates may lead to low interstitial levels but result in precipitates. A clean ferrite has superior ductility, believed to be an important factor in obtaining the dual phase properties.

The addition of substitutional solute atoms are beneficial to the properties of dual phase steels since they increase the strength proportionally more than they decrease ductility. Elements such as silicon and phosphorus give the maximum increase in strength per unit concentration. However, this

effect should be viewed in conjunction with ductility. Maushi and Takeshi[44] found that substitutional strengthening by silicon and manganese resulted in the best combination of strength and ductility. Davies[17] determined the UTS and n-values for pure iron solid solution strengthened by silicon and phosphorus for a number of grain sizes. His results showed that a good combination of strength and ductility is obtained by Si-additions, 2% giving better values than 1%, and that phosphorus (0.2 and 0.4% P were studied) gives worse combination.

In a study[45], it is shown that slower cooling after intercritical annealing may enable austenite pool first to decrease in size by epitaxial ferrite growth on retained ferrite (ferrite present at the intercritical temperature). The ferrite formed in this manner is referred as epitaxial ferrite. It is found that retained ferrite exhibits, in comparison to epitaxial ferrite, a lower ductility and higher strength that must be accounted for by microstructural differences. Huppy et al.[45] showed that a precipitate structure develops in the retained ferrite during the intercritical annealing. On subsequent cooling, precipitate-free epitaxial ferrite is formed which is expected to have a higher ductility and lower strength than the corresponding retained ferrite. These results suggests that the volume fraction of epitaxial ferrite will be more important in optimizing ductility in dual phase steels.

A study[46] of fatigue behavior of these steels shows that at higher strain amplitudes, the dual phase condition is better than the standard condition. This is to be expected

since high strain amplitude life is controlled by the ductility
of the material and dual phase structures have high ductility.
In low strain amplitude fatigue life region which is controlled
by the yield stress of the material, the standard condition has
as would be expected, better fatigue life than the dual phase
material.

Further, it is proved that dual phase steels are considerably tougher than conventional HSLA steels.[13] Two possible
explanations are given for this toughness improvement:

(i)   martensite is coherent with ferrite matrix unlike the
      carbides in HSLA steels, and

(ii) the ferrite in dual phase structure has a low strength
      and is tough (resistance to crack propagation) whereas in
      conventional steel the ferrite is strengthened by carbo-
      nitrides precipitates[9] which in general degrade impact
      properties.

The formability of the dual phase steels has also been
studied[47] by determining forming limit diagrams (FLD), limiting
dome height(LDH), stretch bend test and the hole enlargement
tests. It is proved that formability of dual phase steels is
superior to that of the micro-alloyed steel, even though it
falls short of that of the low carbon steel.

2.4   Influence of Heat-Treatment Parameters and Alloying Elements on the Microstructure:

The actual heat-treatment cycle followed for a dual
phase steel depends on the starting microstructure and composition.

2.4.1 Annealing Temperature and Cooling Rate:

Dual phase steels are normally obtained by annealing in the austenite plus ferrite range. Quenching does not give time for diffusion controlled transformations to take place and thus produces volume fractions of polygonal ferrite and martensite according to the equilibrium between ferrite and austenite at the annealing temperature. From this it follows that the volume fraction of martensite in the microstructure increases gradually with intercritical temperature. As the cooling rate is raised there will be a gradual increase in martensite content in microstructure. As the annealing temperature is raised above A_3, the austenite would at a given temperature contain less carbon compared to the situation after intercritical annealing and exhibits therefore a larger tendency to transform to pearlite. In agreement with this VAN-QN steel has been found to form pearlite more easily when annealed above A_3 than below.[39]

2.4.2 Initial Microstructure:

A fine initial microstructure ascertains a finer structure after anneal.[39] In order to assure that pearlite formation is avoided, or more generally expressed that a sufficient hardenability is attained a complete dissolution of the cementite is essential during the anneal. With the short annealing time, desired in production, it is therefore, important to have an initial structure of fine cementite in order to get a short time for dissolution.

2.4.3 Alloying Elements:

The composition of a dual phase steel must be such that the desired microstructure can be easily produced even with some variations in the thermomechanical processes inherent in commercial production. In other words, the steel should have sufficient hardenability. Silicon is considered to be important in creating correct structure because of its tendency to retard cementite formation and thereby probably also pearlite formation. Manganese tends to produce a finer grain size in the transformation products.

Vanadium refines the ferrite grain size but, in solution, can contribute to the hardenability of the austenite. The exact role of vanadium in dual phase steels is not clear. Vanadium suppresses the formation of both ferrite and pearlite.[11] Vanadium in solution reduces the interstitial content of ferrite.[13]

2.5 Review of Deformation Models for Dual-Phase Steels:

Several theoretical treatments of deformation and fracture in multiphase system have been employed to relate strength and ductility to volume fraction of martensite in dual phase steels. All the theoretical treatments of deformation behaviour of dual phase steels assume that the microstructure can be modelled as a composite material consisting of a hard phase (martensite) and a soft phase (ferrite). The differences in the various approaches arise primarily from the nature in which the strain is assumed to partition between the two phases

and from the manner by which one phase affects the flow characteristics of the other phase.

2.5.1 Continuum Mechanics Models:

2.5.1.1 Isostrain Assumption:

In a series of papers[13-17], Davies has made use of rule of mixture to partition stresses combined with deformation model of Mileiko[18]. Main assumptions of this theory are

(1)   equal strain in both phases

(2)   stress-strain relationships for two phases obey

$$\sigma = K \varepsilon^n$$

By applying realistic values of n and K for ferrite and martensite and assuming that uniform strains of two phases are independent of their tensile strengths, Davies has calculated the uniform elongation as function of tensile strength of the steel for various tensile strengths of the ferrite and the martensite. The conclusions to be drawn from this is that at the desired strength of dual phase steel:

(i)   uniform elongation of the steel increases with the UTS of ferrite

(ii)   uniform elongation of steel increases with the UTS of martensite

(iii)   a larger increase in uniform elongation is gained by increasing the strength of ferrite than increasing the strength of martensite at a given strength level of steel.

(iii) is more significant result since it can guide a metallurgist in the common situation where he has to make choice

between two possibilities which cannot be attained at the same time.

2.5.1.2 Strain Partitioning Models: However, as has been discussed by Ostrom and Lindgren[39] the assumption of equal strain in two phases is most certainly not fulfilled in dual phase steels. Instead, there is a partition of strain as well as of the stress, between the ferrite and martensite such that the strain is considerably lower in harder component than in the softer. Comparing its results with the results of the equal strain model gives for equivalent properties of the components, that it is now more favourable to increase the martensite strength than ferrite strength, hence opposite to the results obtained from equal strain model. A further comparison of the two models showed that they both predict, in agreement with experimental findings, a linear relationship between the tensile strength and volume fraction of martensite. Another model due to Araki et al.[48] used a continuum mechanics approach which evaluates the internal stored energy of the two phases and the composite. Strains were partitioned according to the rule of mixture. With this analysis again the tensile strength was found to have linear dependence with volume fraction of martensite.

Tamura et al.[20] reasoned that actual tensile behaviour lies between the conditions of isostrain and isostress. The ratio of the strain in martensite to that in ferrite, m, was assumed to be constant with the limits of $m = 1$ for an isostrain condition and $m = 0$ for an isostress condition. Based on a deformation model dependent on magnitude of m, stress-strain

curves were developed for values of m in between 0 and 1. With Tamura's model, Speich and Miller[19] found that a value of m = 0.01 was appropriate for a series of dual phase steels with various carbon contents.

2.5.2. Micro-mechanical Model:

Other investigators[49,50] have developed models in which the stress state within each phases is not assumed to be constant as in the continuum approaches described above. For instance in the micro-mechanistic model developed by Ashby[50] and applied to dual phase steels by Ramos et al.[51], the martensite is assumed to be non deforming and dislocations accumulate to accommodate the plastic strain gradients which result from the non-homogeneous deformation. The strengthening effect of these dislocations in the ferrite depends on their mean free path which is a function of volume fraction of martensite and its size. According to this theory, the work hardening rate of dual phase steel dependence on the parameters $\sqrt{f/d}$, where f is volume fraction of second phase and d is the mean second phase island diameter.[52]

Although these viewpoints undoubtedly are of value in designing dual phase steels it has to be recognized that many aspects of great importance for the properties are not contained in these models. Furthermore, the models overlook entirely the distribution of the phases in the microstructure, clearly the number, shape and size of the martensite will affect the properties of steel significantly.

2.6 Investigation of Bauschinger Effect in Dual Phase Steels:

Bauschinger effect can be defined simply as the phenomenon whereby the plastic flow stress for the deformation of a material in reverse direction is lower than that in original direction. Obviously this effect is important in forming processes which involve a reversal in deformation mode.

One of the earliest dislocation concepts[53] to explain this behaviour was the idea that dislocations pile-up on slip planes at barriers in the crystal. The pile-ups produce a back stress which opposes the applied stress on the slip plane. An explanation of Bauschinger effect is that the back stress developed as a result of dislocation piling up at the barriers during the first loading cycle is aiding dislocation movement when the direction of slip is reversed. Furthermore, when the slip direction is reversed, dislocations of opposite sign could be created at the same sources that produced the dislocations responsible for strain in the first slip direction. Since dislocations of opposite sign attract and annihilate each other, the net effect would be a further softening of the lattice.

Another mechanism of Bauschinger effect lies in the structure of cold worked state. During plastic deformation dislocations will accumulate at /barriers in tangles, and eventually form cells. Now, when load is removed, the dislocation lines will not move appreciably because the structure is mechanically stable. However, when the direction of loading is reversed, some dislocations lines can move an appreciable distance at a low shear stress because the barriers to the rear of dislocations

are not likely to be so strong and closely spaced as those immediately in front.

Bauschinger behaviour has been studied extensively in single phase metals and alloys.[54] In a two ductile phase alloy, plastic deformation occurs inhomogeneously due to the difference in flow stress between two component phases.[55] Therefore, compared with a single phase alloy, the distribution of dislocations in plastically deformed two ductile phase alloy seem to be quite inhomogeneous, so that a large Bauschinger effect is expected to occur. However, this effect of two-ductile-phase alloys has not been examined well except in ferrite-pearlite carbon steels.[56] The flow stress of alloys containing two-ductile-phase is influenced by the volume fraction of hard phase, shape of grains of hard phase and the yield strength ratio of hard phase to that of soft phase.[57]

CHAPTER III

EXPERIMENTAL PROCEDURE

The various procedures with their relevant experimental details regarding the (i) material preparation, (ii) heat treatment, (iii) metallography and (iv) mechanical testing are presented in this chapter.

3.1 Materials:

The compositions of the steels used in this investigation are shown in Table 3.1.

Table 3.1

Compositions of steels

Alloy No	Weight percentage of elements					
	C	Mn	Si	S	P	V
1	0.13	0.51	1.48	0.027	0.011	0.085
2	0.11	0.97	1.51	0.019	0.013	0.080
3	0.11	1.46	0.47	0.014	0.013	0.090
4	0.12	1.55	0.89	0.022	0.014	0.087

These alloys were prepared in a vacuum induction furnace. All the heats were deoxidised by aluminium shots. The cross sectional area of each ingot was initially 12 cm x 12 cm. These ingots were forged into the rods of square cross section of 25 mm x 25 mm .

The tensile, impact and tension-compression test specimens of standard dimensions as illustrated in Figure 3.1 were prepared from these forged square bars. Specimens for optical microscopy were cut from the specimens used for impact testing.

3.2 Heat-Treatment:

All the samples were coated suitably with a ceramic powder so as to prevent oxidation during heat-treatment.

The heat-treatment was given in two stages, (i) austenitizing and (ii) intercritical annealing. All the samples were austenitized for 30 minutes at four different temperatures, viz. 880, 910, 940 and 970°C and then aircooled. The purpose of choosing different austenitizing temperature was to produce varying size of ferrite grains.

The austenitized samples were held in the two phase field (ferrite plus austenite) for 30 minutes and then water-quenched. The four intercritical annealing temperatures viz. 750, 770, 790 and 810°C were selected so as to attain the different volume fractions of martensite.

3.3 Optical Metallography:

Conventional optical metallography was used to examine the microstructure of each heat-treated specimen. These were etched by 4% picral for 15 minutes and metallurgical microscope was used to photograph the etched surfaces at a magnification of 300X.

The volume fraction of each heat-treated specimen was calculated from photomicrographs by point-count method using a

5 mm square grid. An average of approximately 1000 counts
were made for each case. The grain-size measurement was done
for the specimens austenitized at 860 and 970°C and intercriti-
cally annealed at 750 and 810°C using linear intercept method.

3.4 Mechanical Testing:

The procedures used for tensile, impact and tension-
compression testings are given below in this section.

3.4.1 Tensile Testing:

The standard tensile specimens (Figure 3.1a) were used
for the test. The tensile tests were performed at room temper-
ature using an Instron (Model 1195) machine with a cross-head
speed of 0.5 mm/minute, a chart speed of 20 mm/minute and a
full-scale load of 5000 Kgs. From the charts 0.2% and 1% proof
stress, ultimate tensile strength and total,   uniform elong-
ation were calculated.

True stress and true strain curves were plotted to
calculate the work hardening coefficient 'n'. For this purpose,
the X and Y co-ordinates were measured from the load-elongation
chart for a strain increment of 0.0089 and a suitable computer
program was developed to analyse the data thereby calculating
the true stress and true-strain values for each strain increment.
The ln σ (true stress) vs. ln ε (true strain) curves were
plotted. The slope of these curves give the value of 'n' for
each specimen.

3.4.2 Impact Testing:

The standard V-notched charpy specimens (Figure 3.1b) were tested at room temperature to determine the impact strength using an Avery model machine and impact values were directly read on the scale in terms of Kg-m.

3.4.3 Tension-Compression Test:

This test was done to observe Bauschinger effect. The standard honr glass type samples (Figure 3.1c) austenitized at 970 and 880°C and intercritically annealed at 750 and 810°C were used for these tests. The tension-compression tests under load control mode were carried out on an MTS machine using the diametrical extensometer. The details of the test are as follows:

Load range $= 50\%$ i.e. 5 T $= 10$ V (300 sec)

Extensometer range $= R_4$ i.e. 10 V $= 0.20$ mm

X-Recorder setting in tension cycle $= 1$ V/cm

X-Recorder setting in compression cycle $= 0.1$ V/cm

Y-Recorder setting $= 0.5$ V/cm

Four tension-compression cycles at 0.2, 5, 10 and 15 percent tensile prestrain levels were performed on each specimen at room temperature. In compression cycle, only 0.2% strain was given in each cycle. The area under tension and compression curves was measured with a planimeter. Bauschinger parameters were calculated by using the formula given below with reference to Figure 3.2.

$$(1) \quad \sigma_B = \sigma_P - \sigma_R$$

$$(2) \quad \beta_\sigma = \frac{(\sigma_P - \sigma_R)}{\sigma_P}$$

$$(3) \quad \beta_\varepsilon = \frac{\varepsilon_B}{\varepsilon_P}$$

$$(4) \quad \beta_E = \frac{E_S}{E_P}$$

where,

σ_P = tensile prestress

σ_R = 0.2% offset yield strength in compression

ε_B = Bauschinger strain at 0.5 σ_P

ε_P = Tensile prestrain

E_S = Energy saved in reversed cycle

E_P = Energy associated with tensile prestrain

β_σ = Bauschinger stress parameter

β_ε = Bauschinger strain parameter

β_E = Bauschinger energy parameter.
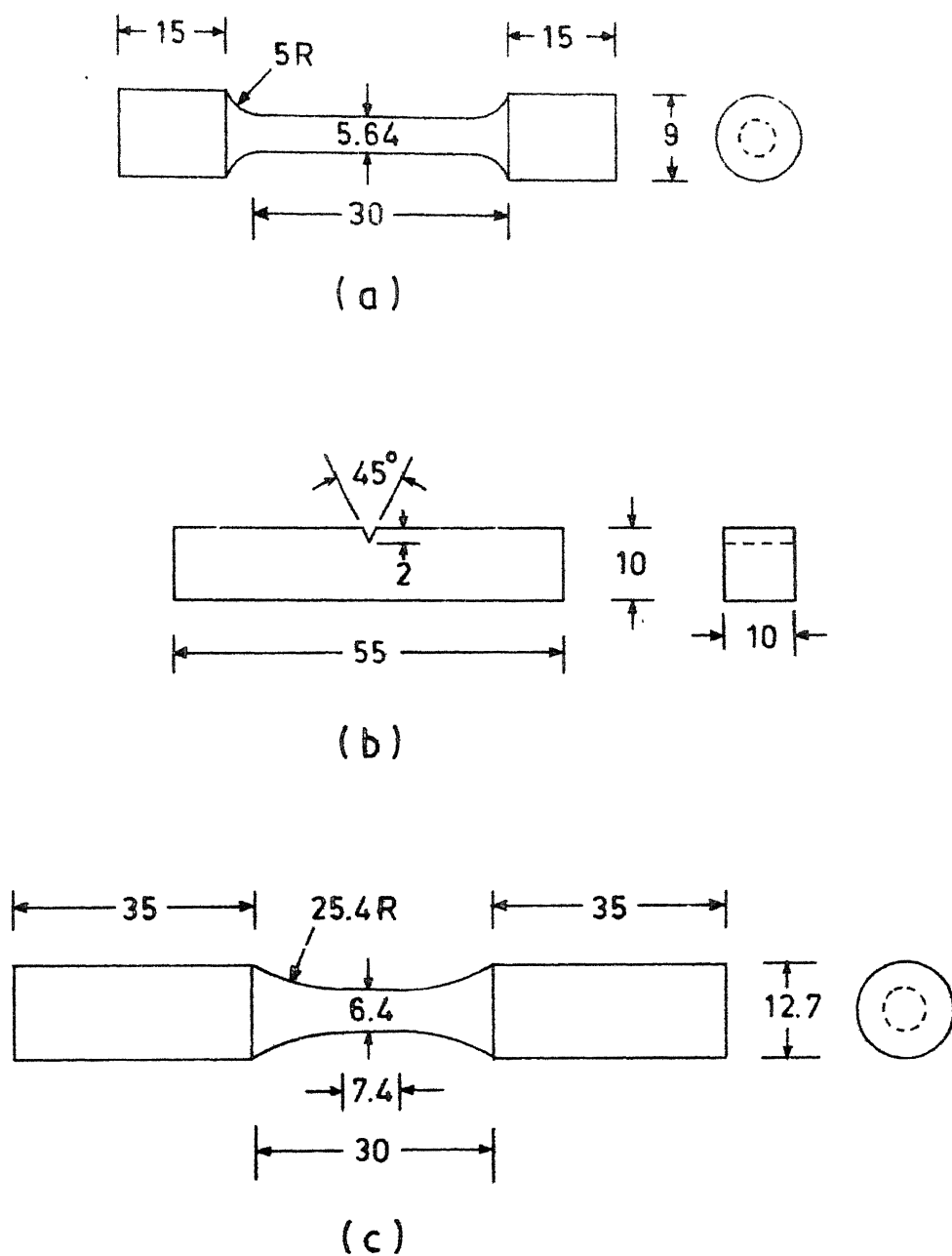
Fig. 3.1. SKETCHES SHOWING TYPICAL DIMENSIONS OF
(a) Tensile specimen, (b) harpy specimen and
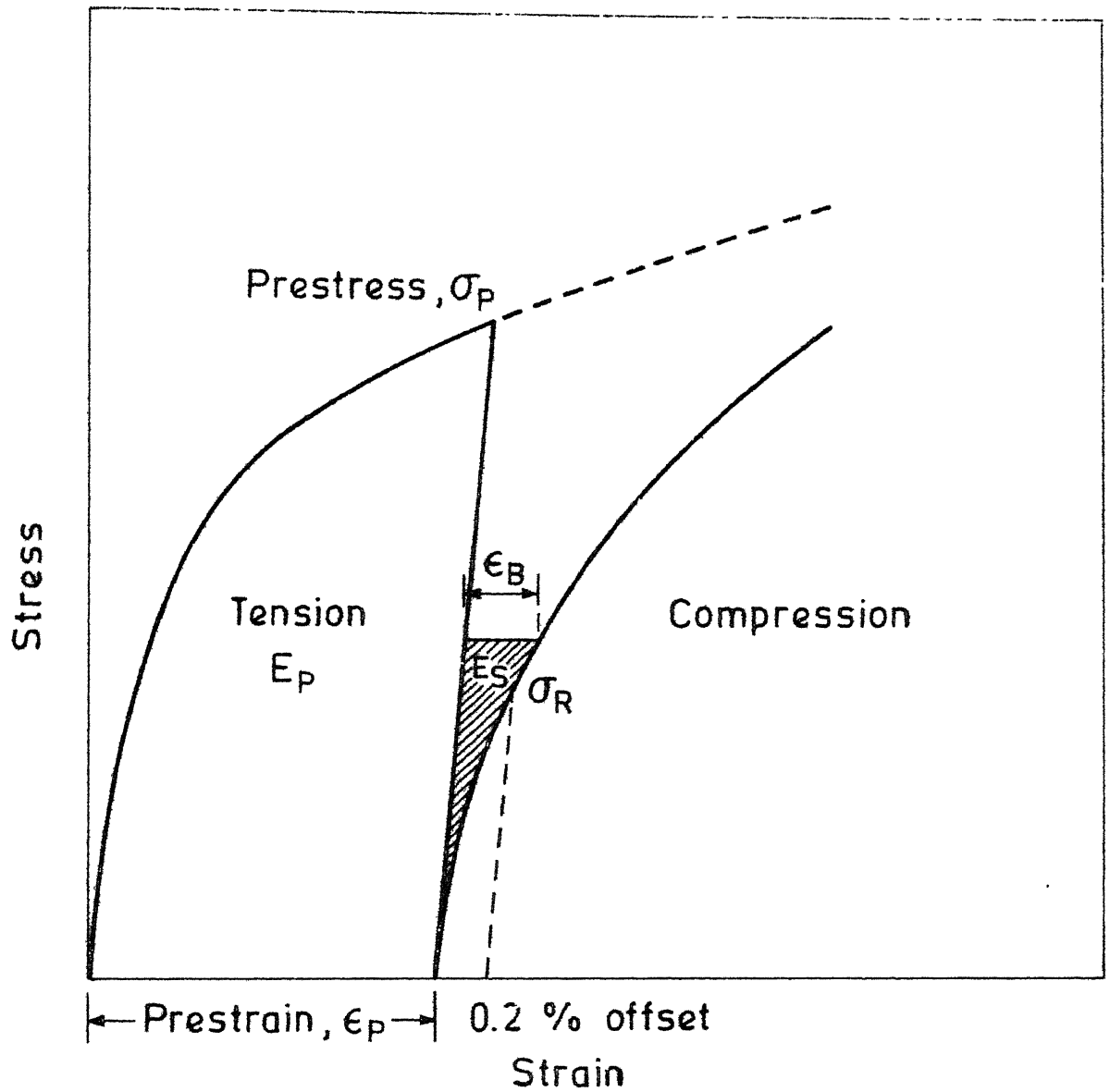(c) Tension-compression te specimen.

FIG. 3.2. SCHEMATIC DIAGRAM OF THE BAUSCHINGER EFFECT.

CHAPTER   IV

EXPERIMENTAL   RESULTS

4.1 Microstructural Observations:

The microstructures observed at different austenitizing and intercritical temperatures are shown in Figures 4.1(a-d), 4.2(a-d), 4.3(a-d) and 4.4(a-d) for alloys 1, 2, 3 and 4 respectively. It is clear that in all cases, dual phase structure is produced. These microstructures suggest that globular martensite is formed along ferrite grain-boundaries.

The volume fraction of martensite present in specimens heat-treated at different temperatures are shown in Table 4.1. The variation of volume fraction of martensite with intercritical temperature at an austenitizing temperatures of 970°C is shown graphically in Figure 4.5. In all the cases the volume fraction of martensite is observed to increase with intercritical temperature. Further, it is clear that alloys 3 and 4 have somewhat higher volume fraction of martensite than alloys 1 and 2. Austenitizing temperature does not seem to affect martensite content.

It is seen from Table 4.2 that in all the cases, the ferrite grain size is smaller in specimens which were annealed at an intercritical temperature of 810°C in comparison to that of intercritical temperature of 750°C for a given austenitizing temperature. Further, Table 4.2 suggests that ferrite grains are coarser in specimens annealed at higher austenitizing

temperature for a given intercritical temperature. The grain size of alloys 1 and 2 is slightly coarser than that of alloys 3 and 4.

4.2 Tensile Test Results:

The tensile test results are shown in Tables 4.3, 4.4, 4.5 and 4.6 for alloys 1, 2, 3 and 4 respectively. Typical true stress-true strain curves at the austenitizing temperature of 970°C are shown in Figures 4.6, 4.7, 4.8 and 4.9 for different alloys of the present study.

0.2% offset yield and ultimate tensile strength of different alloys are shown in Figure 4.10 as a function of intercritical temperature for a given austenitizing temperature of 970°C. Yield strength of alloy 1 is not much dependent on intercritical temperature whereas the yield strength of the other alloys shows a tendency to increase with intercritical temperature. Alloy 3 shows an increasing tendency of yield strength with decrease in austenitizing temperature whereas the yield strength of alloys 1, 2 and 4 is not much affected by austenitizing temperature.

Further, it is seen that ultimate tensile strength increases with intercritical temperature in all alloys. The ultimate tensile strength increases slightly with decrease in austenitizing temperature in alloys 1 and 3 whereas the same trend is absent in alloy 2 and 4.

The variation of total and uniform elongation with intercritical temperature at austenitizing temperature of 970°C is shown in Figure 4.11. It may be noted that ductility is

impaired with intercritical temperature in all cases. Ductility is not significantly affected by austenitizing temperature. The work hardening coefficient (Tables 4.3, 4.4, 4.5 and 4.6) is also observed to decrease with intercritical temperature for alloys 2, 3 and 4 whereas there is no significant change in work hardening coefficient 'n' of alloy 1 with intercritical temperature. Typical $\ln(\sigma)$ vs. $\ln(\varepsilon)$ curves for different alloys are shown in Figure 4.12. Work hardening coefficient is found to be constant over the whole strain range.

4.3 Impact Test Results:

Impact toughness data of different alloys are shown in Tables 4.3, 4.4, 4.5 and 4.6. The dependence of impact toughness on intercritical temperature at the austenitizing temperature of 970°C is shown in Figure 4.13. In general, there is a slight increase in toughness with intercritical temperature. In alloy 3, this variation is somewhat higher than in other alloys. Austenitizing temperature is not found to affect impact toughness. One striking observation is that the toughness of alloy 3 is significantly higher than that of other alloys.

4.4 Tension-Compression Test Results:

The Tables 4.7, 4.8, 4.9 and 4.10 show the Bauschinger effect obtained from tension-compression tests of alloys 1, 2, 3 and 4 respectively. The variation of Bauschinger stress, strain and energy with percent tensile prestrain are shown graphically in Figures 4.14, 4.15 and 4.16 respectively. It is clear that Bauschinger effect increases with tensile prestrain and

intercritical temperature. In general, the magnitude of Bauschinger effect is slightly more for lower austenitizing temperature. Further it may also be noted that the magnitude of Bauschinger effect in alloys 3 and 4 is higher than that of alloys 1 and 2.

Bauschinger parameters are almost constant with tensile prestrain. Values of Bauschinger parameter are observed to increase slightly with intercritical temperature whereas austenitizing temperature does not have any effect.

Table 4.1

Variation of martensite content with heat-treatment

Alloy No.	Austenitizing temperature °C	Volume fraction of martensite (%) at intercritical temperatures			
		750°C	770°C	790°C	810°C
1	880	15	18	23	25
	910	14	15	18	20
	940	11	15	18	19
	970	12	15	18	20
2	880	14	21	20	22
	910	12	15	17	23
	940	12	13	15	22
	970	13	14	16	19
3	880	22	23	26	32
	910	19	21	20	27
	940	18	23	23	26
	970	24	26	29	30
4	880	17	20	24	26
	910	20	23	25	25
	940	22	24	28	29
	970	17	22	25	27

Table 4.2

Variation of ferrite grain size with heat-treatment

Alloy No.	Austenitizing/Intercritical temperature (°C)	Ferrite grain size (μm)
1	880/750	6.5
	880/810	4.0
	970/750	9.0
	970/810	6.5
2	880/750	6.0
	880/810	6.0
	970/750	9.0
	970/810	7.3
3	880/750	4.5
	880/810	3.2
	970/750	6.0
	970/810	4.0
4	880/750	5.0
	880/810	4.0
	970/750	6.5
	970/810	5.0

Table 4.3

Mechanical properties of alloy 1

Austenitizing/ Intercritical temperature (°C)	Tensile properties						Impact tough-ness (N-M)
	0.2% offset yield stren-gth (MPa)	1% offset yield stren-gth (MPa)	UTS (MPa)	Uniform elong-ation (%)	Total elon-gation (%)	Work hardening coeffi-cient 'n'	
880/750	369	417	602	17	25	0.20	235
880/770	388	437	690	16	24	0.22	264
880/790	398	466	719	14	20	0.22	255
880/810	417	485	728	15	20	0.21	294
910/750	310	353	593	20	30	0.24	274
910/770	311	350	670	17	23	0.22	294
910/790	349	408	680	14	18	0.20	294
910/810	350	437	700	15	19	0.22	284
940/750	359	408	580	21	32	0.25	206
940/770	349	409	602	18	24	0.24	225
940/790	350	417	660	17	24	0.23	304
940/810	360	437	709	20	25	0.22	313
970/750	330	360	563	22	30	0.24	196
970/770	331	370	592	20	26	0.23	215
970/790	340	388	651	18	24	0.21	274
970/810	350	427	675	18	23	0.21	284

Table 4.4

Mechanical properties of alloy 2

Austenitizing/ Intercritical temperature (°C)	Tensile properties						Impact toughness (N-M)
	0.2% offset yield strength (MPa)	1% offset yield strength (MPa)	UTS (MPa)	Uniform elongation (%)	Total elongation (%)	Work hardening coefficient 'n'	
880/750	291	326	583	24	29	0.23	284
880/770	350	428	665	23	26	0.22	372
880/790	379	466	670	19	25	0.21	382
880/810	388	495	738	18	21	0.18	392
910/750	301	330	602	25	30	0.25	382
910/770	369	446	680	23	28	0.22	392
910/790	398	495	738	21	26	0.21	441
910/810	427	514	777	18	25	0.22	598
940/750	281	350	583	21	25	0.25	372
940/770	340	417	641	20	23	0.23	372
940/790	350	437	665	18	23	0.23	392
940/810	360	446	660	14	20	0.20	588
970/750	360	427	647	21	27	0.23	314
970/770	380	456	700	19	25	0.22	353
970/790	390	485	728	16	22	0.20	431
970/810	447	505	738	12	20	0.19	470

Table 4.5

Mechanical properties of alloy 3

Austenitizing/ Intercritical temperature (°C)	Tensile properties						Impact tough-ness (N-M)
	0.2% offset yield stren-gth (MPa)	1% offset yield stren-gth (MPa)	UTS (MPa)	Uniform elong-ation (%)	Total elong-ation (%)	Work hardening coeffi-cient 'n'	
880/750	417	466	651	19	25	0.18	1058
880/770	437	505	690	20	26	0.15	1098
880/790	515	612	767	13	20	0.13	1195
880/810	563	660	777	7	12	0.11	1607
910/750	388	456	645	20	27	0.19	1176
910/770	417	485	670	22	27	0.18	1215
910/790	466	544	670	18	27	0.16	1587
910/810	468	553	719	17	26	0.15	1744
940/750	350	398	641	23	30	0.24	1097
940/770	370	446	651	18	25	0.18	1107
940/790	437	495	665	17	24	0.15	1744
940/810	456	544	685	16	23	0.15	1803
970/750	314	360	617	25	31	0.20	980
970/770	378	446	660	21	28	0.20	960
970/790	388	476	662	19	25	0.18	980
970/810	437	515	680	16	21	0.17	1411

Table 4.6

Mechanical properties of alloy 4

Austenitizing/ Intercritical temperature (°C)	Tensile properties						Impact tough- ness (N-M)
	0.2% offset yield stren- gth (MPa)	1% offset yield stren- gth (MPa)	UTS (MPa)	Uniform elong- ation (%)	Total elong- ation (%)	Work hardening coeffi- cient 'n'	
880/750	291	388	684	21	26	0.21	374
880/770	370	501	718	19	25	0.20	422
880/790	398	524	757	16	22	0.20	420
880/810	476	582	778	11	20	0.16	549
910/750	310	388	680	22	29	0.21	392
910/770	417	553	755	16	19	0.18	392
910/790	427	563	757	13	17	0.17	549
910/810	446	573	820	13	16	0.18	666
940/750	301	417	680	25	32	0.24	313
940/770	353	476	685	22	30	0.21	323
940/790	369	485	700	20	29	0.18	529
940/810	388	544	816	16	22	0.17	588
970/750	301	388	660	21	30	0.22	215
970/770	360	485	670	16	23	0.20	255
970/790	370	514	738	18	23	0.17	274
970/810	378	534	796	17	21	0.20	470

Table 4.7

Variation of Bauschinger effect with heat-treatment in alloy 1

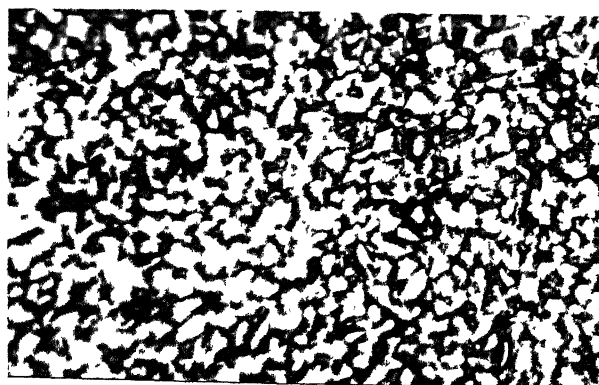| Austenitizing/ Intercritical temperature (°C)	Tensile pre-strain (%)	Bausc- hinger stress (MPa)	Bausc- hinger strain (10^{-3})	Bausc- hinger energy in Joules	Bauschinger parameters		
					Stress	Strain	Energy
	0.2	31	0.40	0.002	0.06	0.01	0.020
880/750	5	209	1.00	0.010	0.34	0.02	0.004
	10	266	1.34	0.010	0.37	0.01	0.003
	15	310	1.59	0.011	0.40	0.01	0.003
	0.2	42	0.06	0.005	0.09	0.03	0.081
880/810	5	462	2.95	0.032	0.58	0.05	0.009
	10	496	3.40	0.036	0.59	0.02	0.005
	15	661	3.50	0.038	0.60	0.02	0.007
	0.2	12	0.44	0.002	0.28	0.07	0.012
970/750	5	200	1.05	0.009	0.36	0.02	0.003
	10	250	1.20	0.010	0.38	0.01	0.003
	15	295	1.40	0.013	0.39	0.01	0.004
	0.2	0	0.19	0.003	0	0.10	0.043
970/810	5	452	3.00	0.026	0.54	0.05	0.008
	10	480	3.20	0.028	0.57	0.03	0.007
	15	598	3.40	0.037	0.58	0.02	0.008

Table 4.8

Variation of Bauschinger effect with heat-treatment in alloy 2
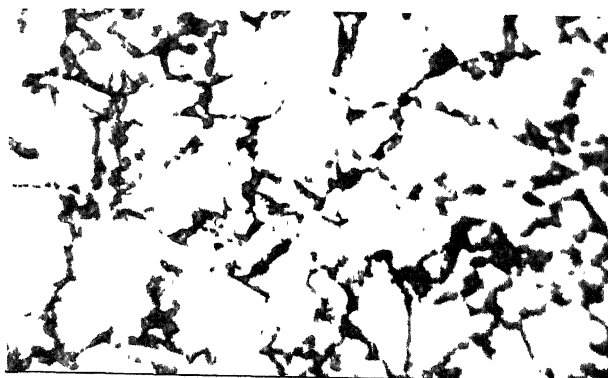
Austenitizing/ Intercritical temperature (°C)	Tensile pre-strain (%)	Bausc-hinger stress (MPa)	Bausc-hinger strain (10^{-3})	Bausc-hinger energy in Joules	Bauschinger parameters		
					Stress	Strain	Energy
880/750	0.2	8	0.19	0.003	0.02	0.09	0.054
	5	398	3.00	0.025	0.54	0.05	0.008
	10	450	3.32	0.027	0.59	0.03	0.010
	15	530	3.56	0.029	0.60	0.02	0.009
880/810	0.2	0	0.19	0.003	0	0.09	0.057
	5	498	3.00	0.041	0.61	0.05	0.012
	10	561	3.50	0.052	0.61	0.04	0.011
970/750	0.2	25	0.13	0.004	0.07	0.09	0.030
	5	344	2.40	0.019	0.51	0.04	0.008
	10	446	2.96	0.023	0.55	0.02	0.009
	15	498	2.97	0.030	0.56	0.01	0.010
970/810	0.2	28	0.30	0.013	0.06	0.01	0.010
	5	442	2.50	0.025	0.56	0.05	0.009
	10	542	3.00	0.030	0.59	0.03	0.008
	15	598	3.32	0.037	0.60	0.02	0.010

Table 4.9

Variation of Bauschinger effect with heat-treatment in alloy 3

Austenitizing/ Intercritical temperature (°C)	Tensile pre-strain (%)	Bausc-hinger stress (MPa)	Bausc-hinger strain (10^{-3})	Bausc-hinger energy in Joules	Bauschinger parameters		
					Stress	Strain	Energy
880/750	0.2	17	0.33	0.004	0.05	0.14	0.050
	5	406	3.47	0.028	0.59	0.06	0.013
	10	470	3.60	0.029	0.60	0.03	0.009
	15	500	3.90	0.030	0.60	0.02	0.009
880/810	0.2	7	0.25	0.034	0.01	0.14	0.056
	5	520	3.96	0.050	0.65	0.08	0.015
	10	606	4.26	0.058	0.66	0.04	0.014
	15	680	4.32	0.059	0.67	0.02	0.013
970/750	0.2	0	0.25	0.003	0	0.12	0.023
	5	385	2.71	0.023	0.58	0.02	0.008
	10	462	2.99	0.025	0.60	0.03	0.007
970/810	0.2	29	0.34	0.015	0.04	0.16	0.010
	5	509	3.57	0.026	0.62	0.06	0.003
	10	555	3.76	0.030	0.61	0.03	0.008
	15	600	3.94	0.036	0.61	0.02	0.001

Table 4.10

Variation of Bauschinger effect with heat-treatment in alloy 4

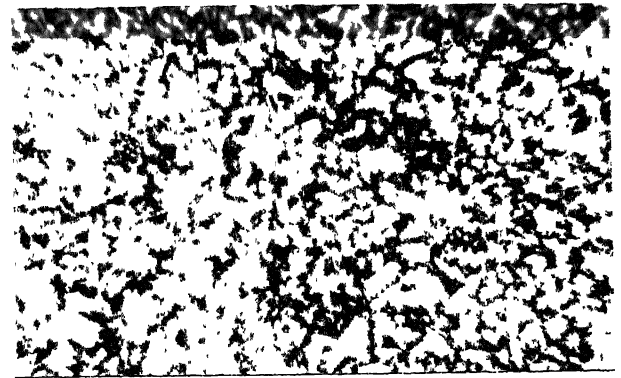| Austenitizing/ Intercritical temperature (°C)	Tensile pre-strain (%)	Bausc- hinger stress (MPa)	Bausc- hinger strain (10^{-3})	Bausc- hinger energy in Joules	Bauschinger parameters		
					Stress	Strain	Energy
880/810	0.2	76	0.18	0.013	0.02	0.18	0.018
	5	509	3.47	0.045	0.62	0.06	0.014
	10	588	3.63	0.056	0.64	0.04	0.013
	15	673	4.00	0.058	0.67	0.03	0.012
970/810	0.2	0	0.94	0.004	0	0.10	0.020
	5	500	3.00	0.018	0.67	0.08	0.005
	10	550	3.47	0.030	0.70	0.04	0.006

(a)
880/750

(b)
880/810
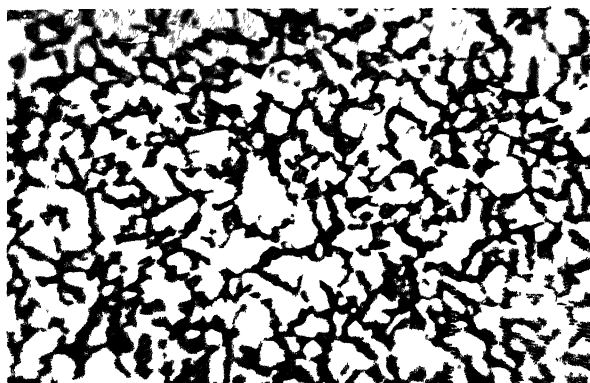
(c)
970/750
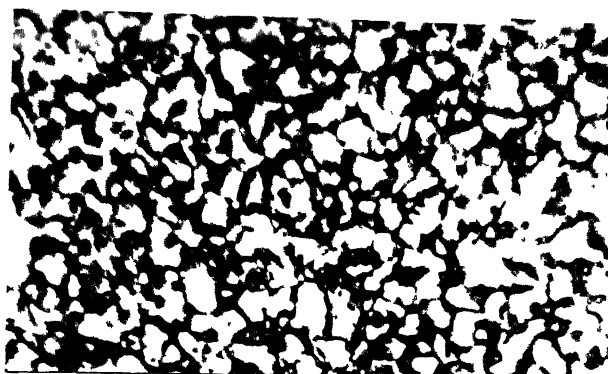
(d)
970/810

Figure 4.1.   Optical micrographs of alloy 1 at austenitizing/
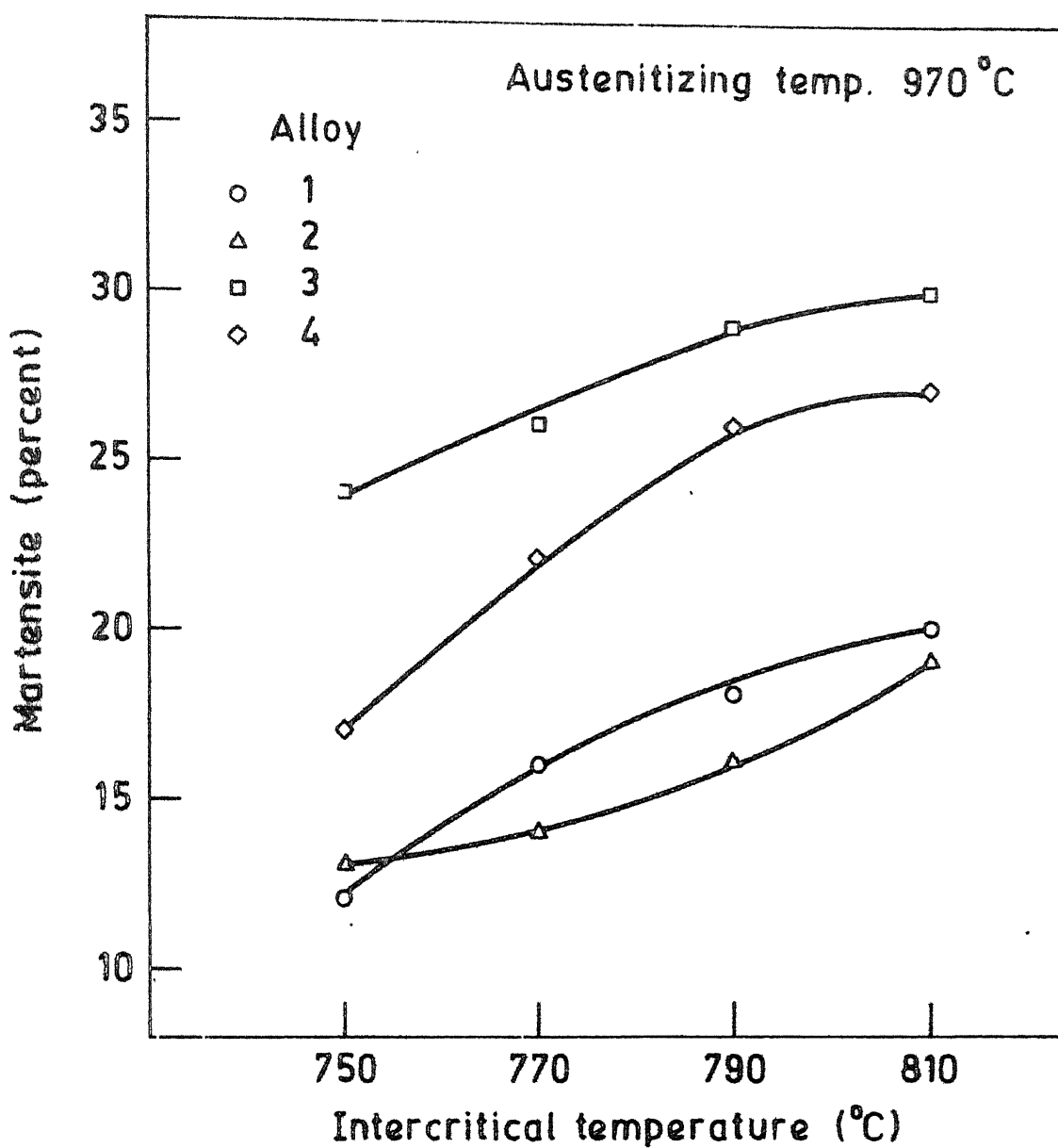intercritical temperature °C.   Mag - 1200X

(a)
880/750

(b)
880/810
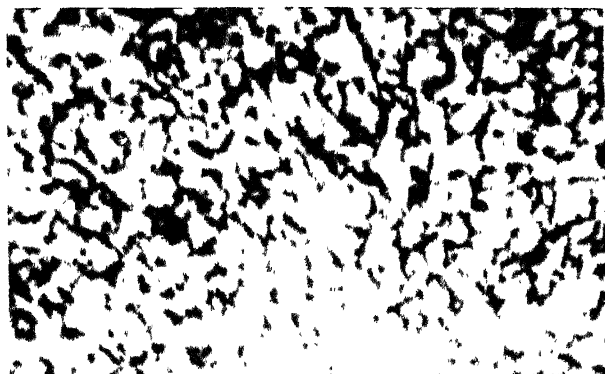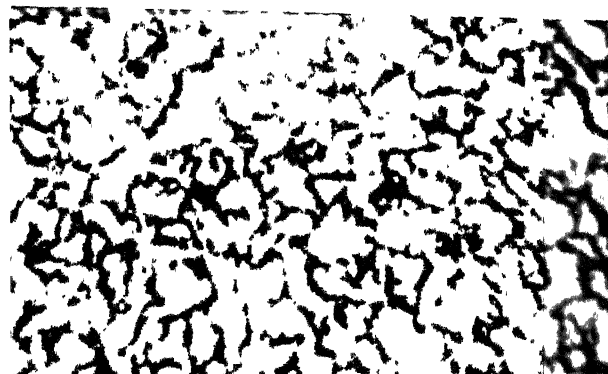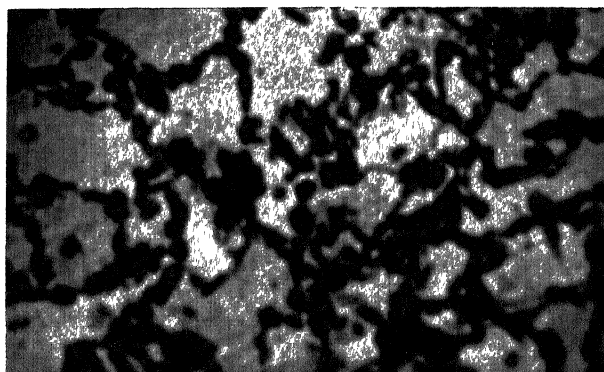
(c)
970/750
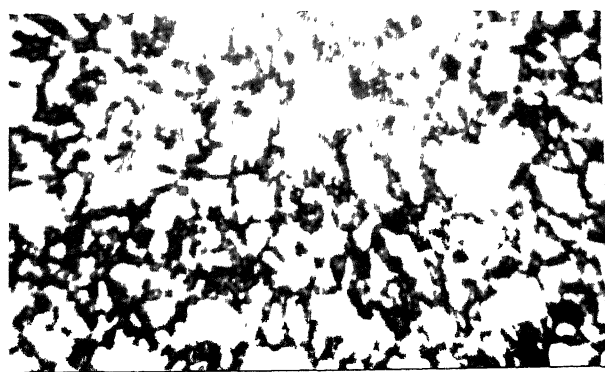
(d)
970/810

Figure 4.2.   Optical micrographs of alloy 2 at austenitizing/
intercritical temperature °C.   Mag - 1200X

<div align="center">

(a)
880/750

(b)
880/810
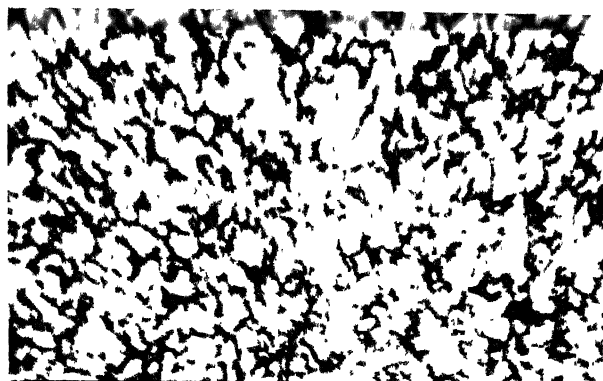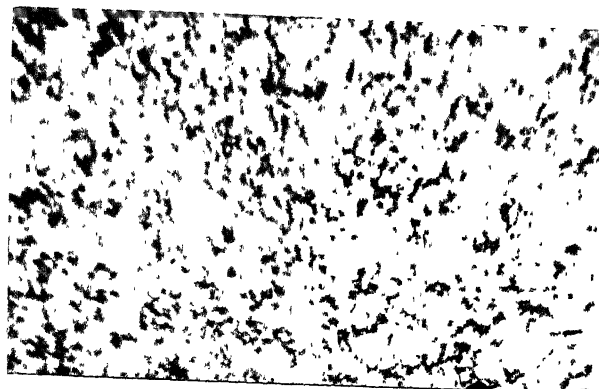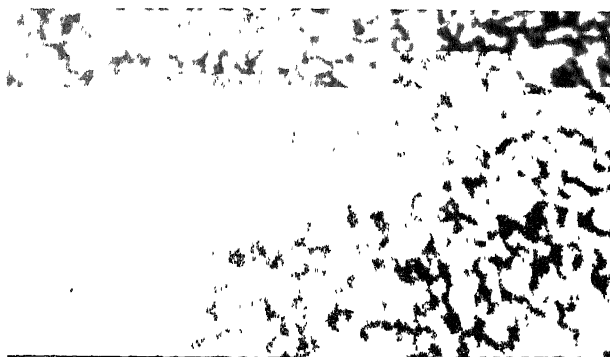
(c)
970/750
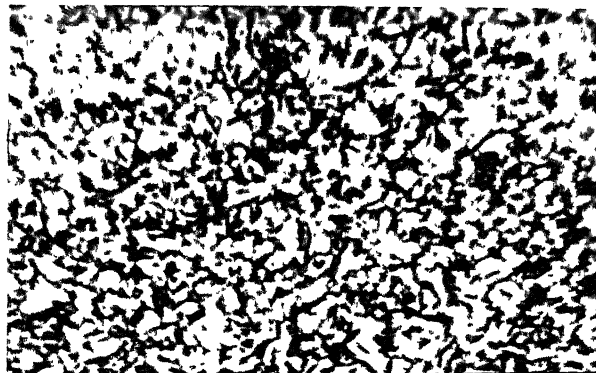
(d)
970/810

</div>

Figure 4.3.   Optical micrographs of alloy 3 at austenitizing/
intercritical temperature °C.   Mag – 1200X

(a)
880/750

(b)
880/810
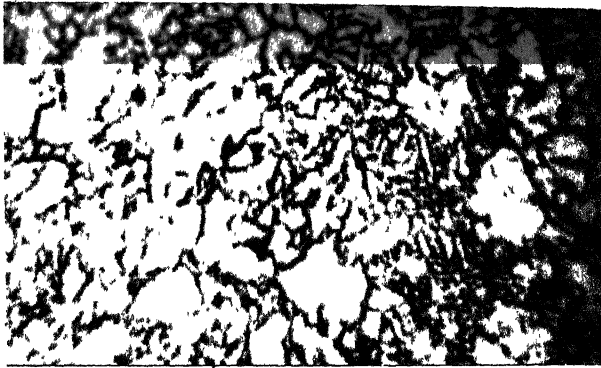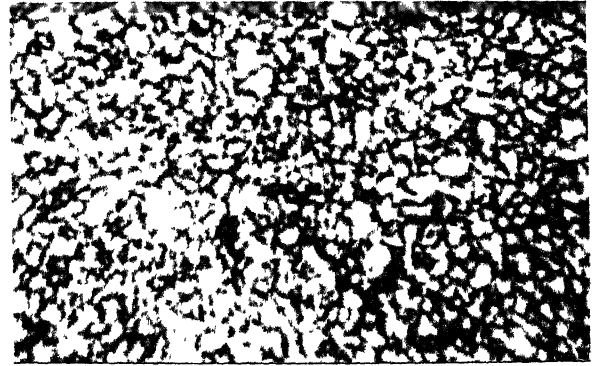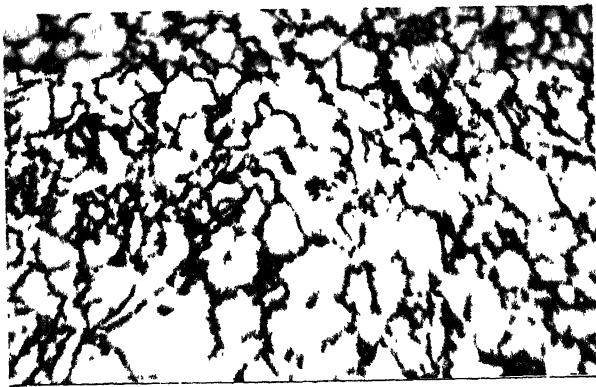
(c)
970/750

(d)
970/810

Figure 4.4. Optical micrographs of alloy 4 at austenitizing/ intercritical temperature °C. Mag - 1200X

FIG. 4.5. EFFECT OF INTERCRITICAL TEMPERATURE ON VOLUME FRACTION OF MARTENSITE.
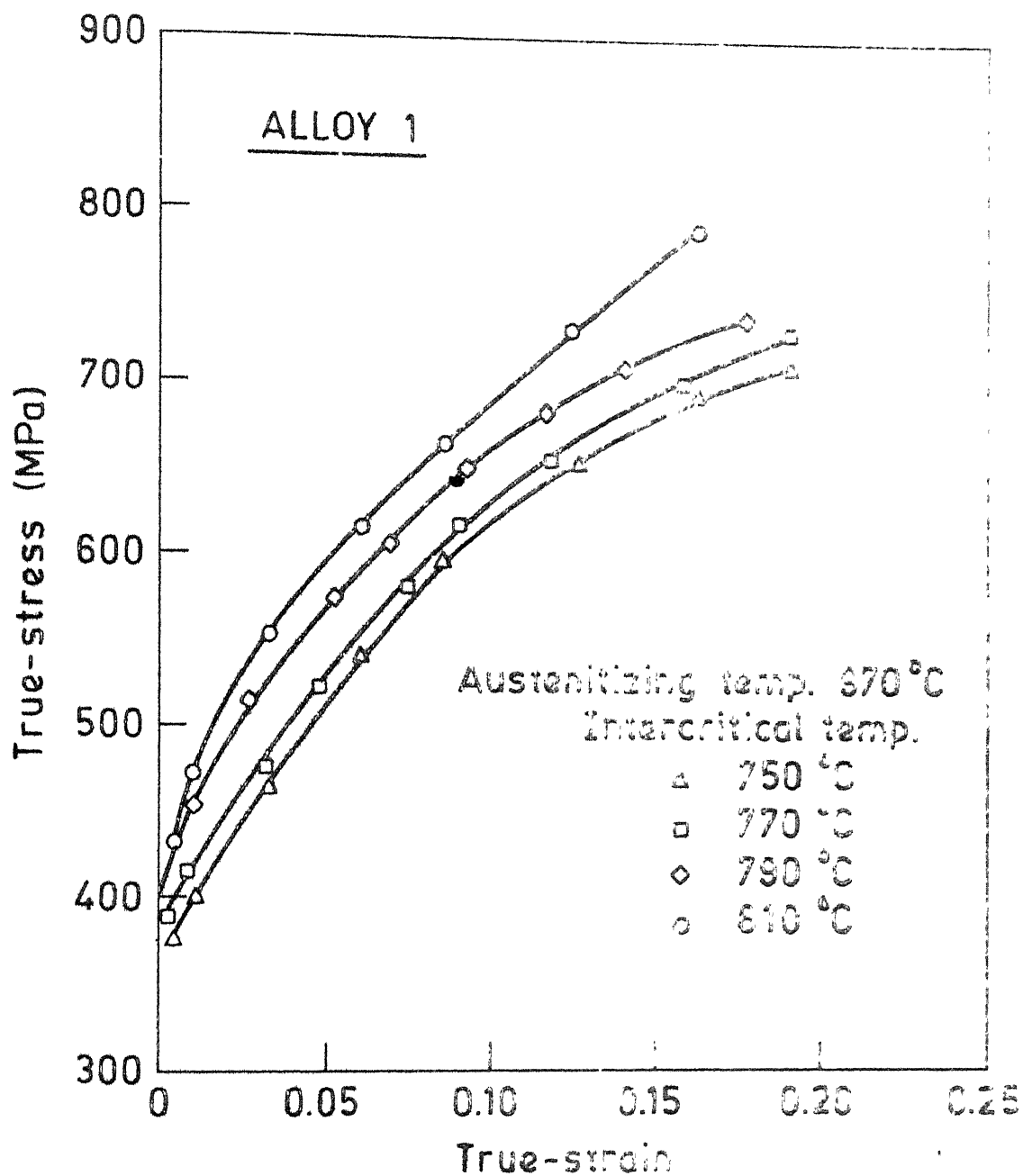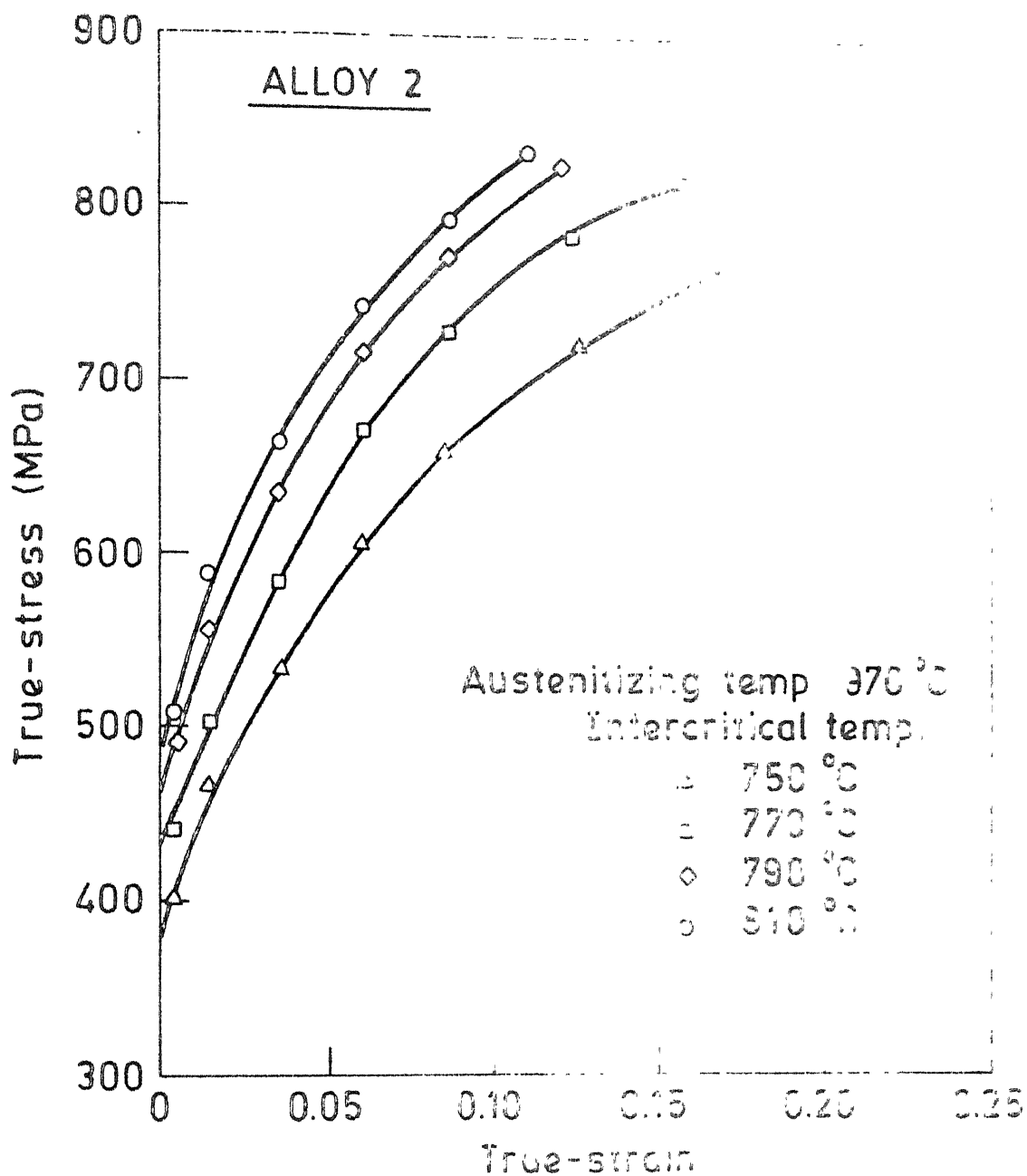
FIG. 4.6. TRUE-STRESS vs TRUE-STRAIN CURVES FOR ALLOY 1.

ALLOY 2

Austenitizing temp 970 °C
Intercritical temp.
□ 750 °C
□ 770 °C
◇ 790 °C
○ 810 °C

FIG. 4.7.   TRUE-STRESS vs TRUE-STRAIN CURVES FOR
ALLOY 2.
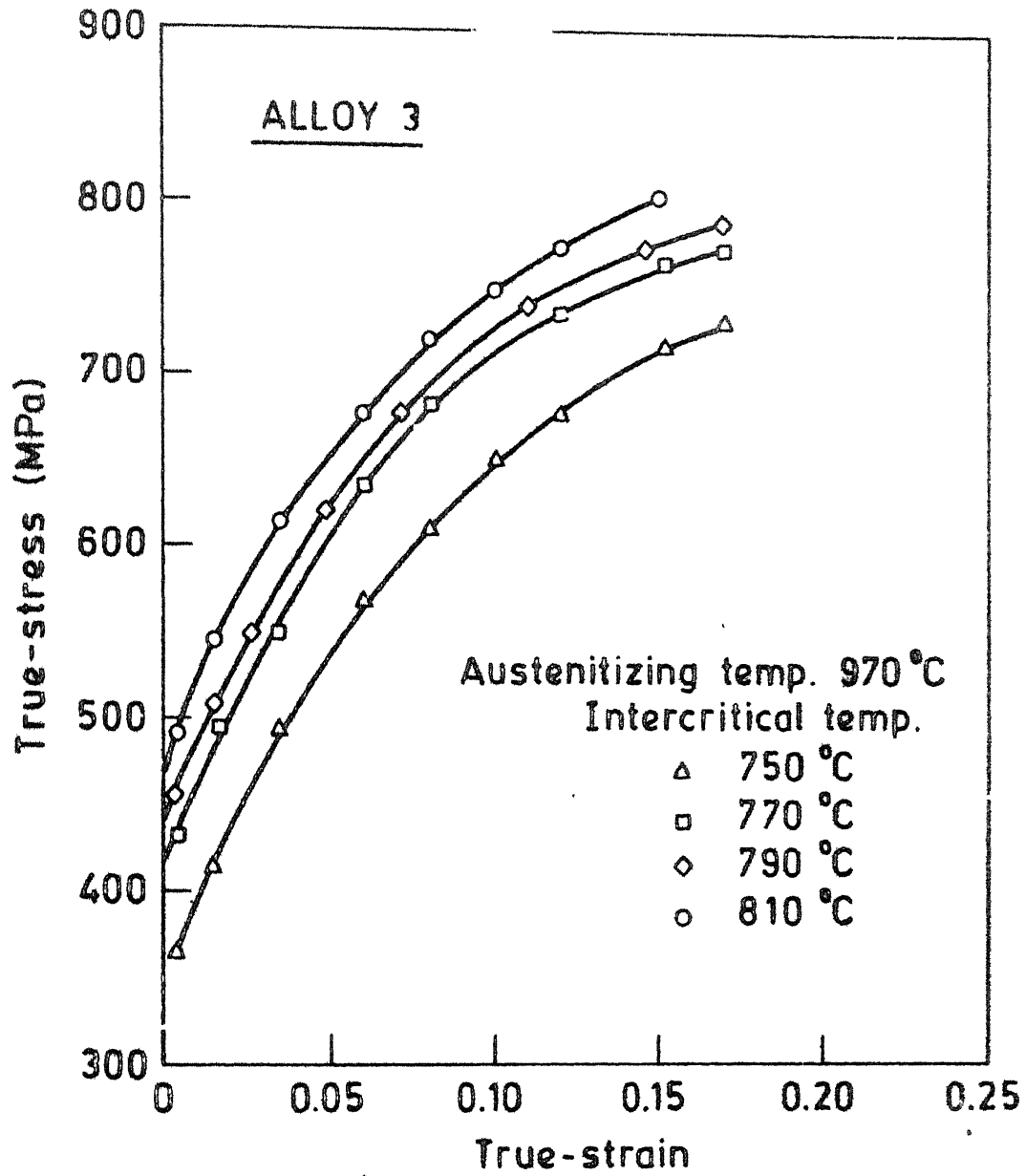
FIG. 4.8. TRUE-STRESS vs TRUE-STRAIN CURVES FOR ALLOY 3.

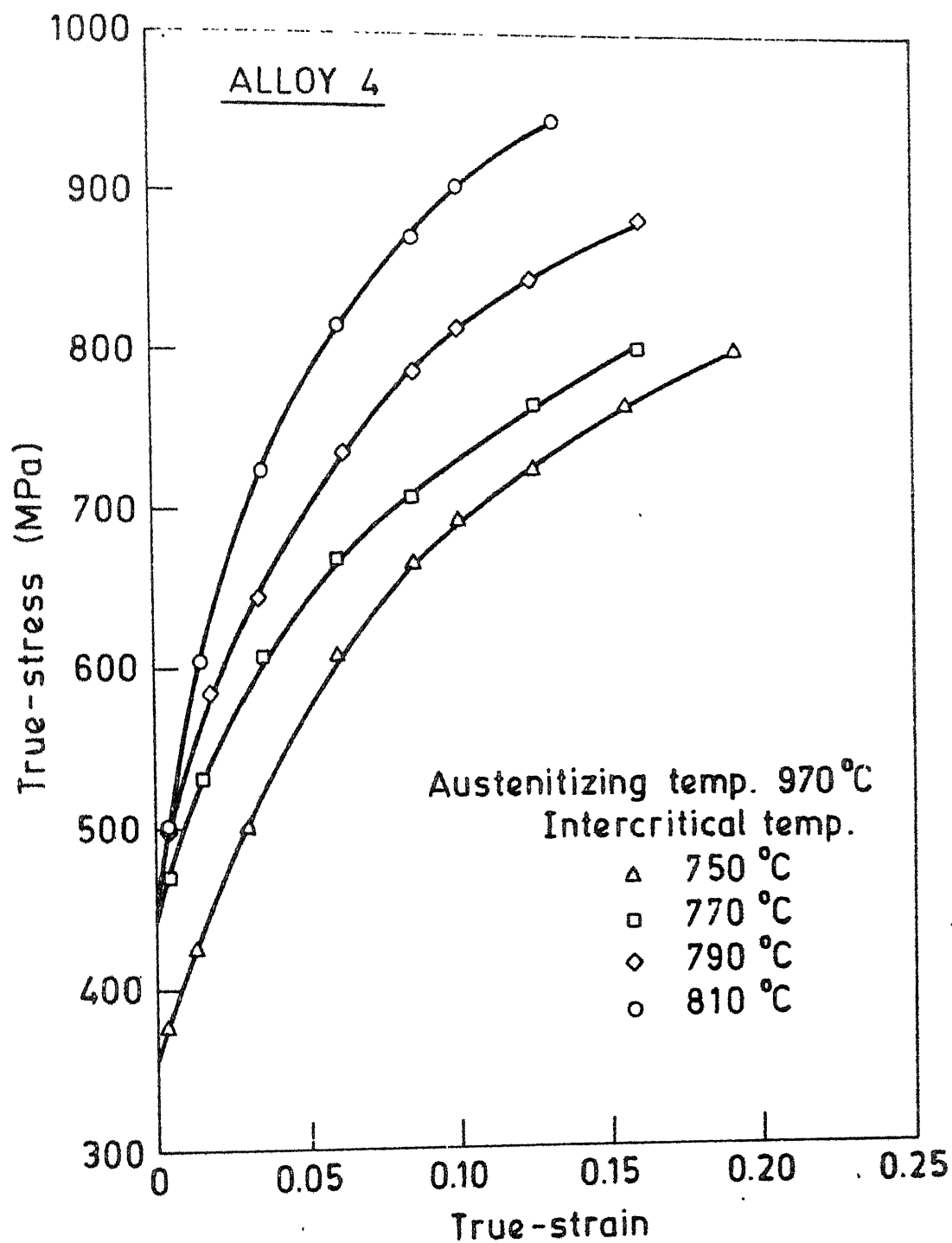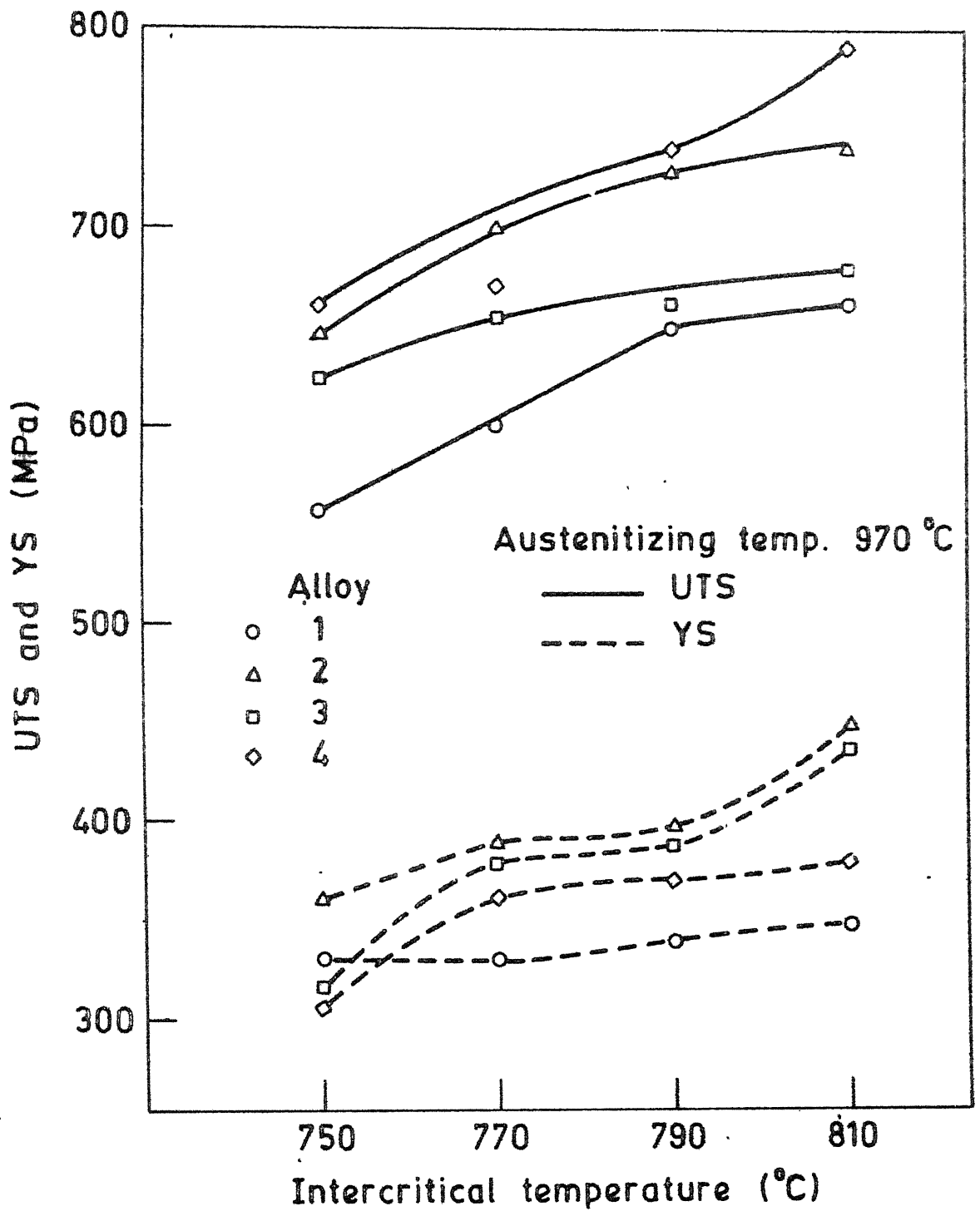FIG. 4.9. TRUE-STRESS vs TRUE-STRAIN CURVES FOR ALLOY 4.

FIG. 4.10. EFFECT OF INTERCRITICAL TEMPERATURE ON UTS
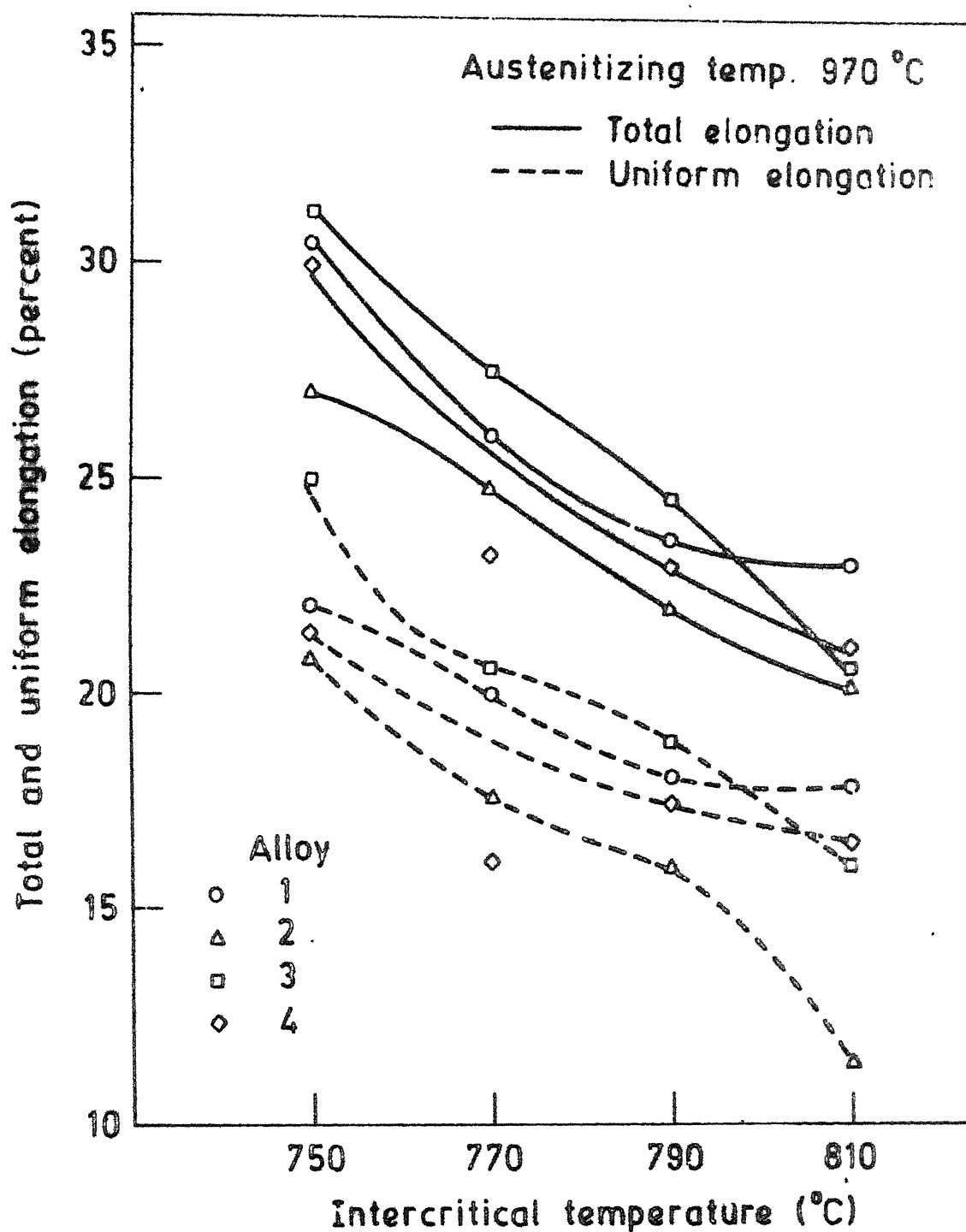AND 0.2 % OFFSET YIELD STRENGTH.
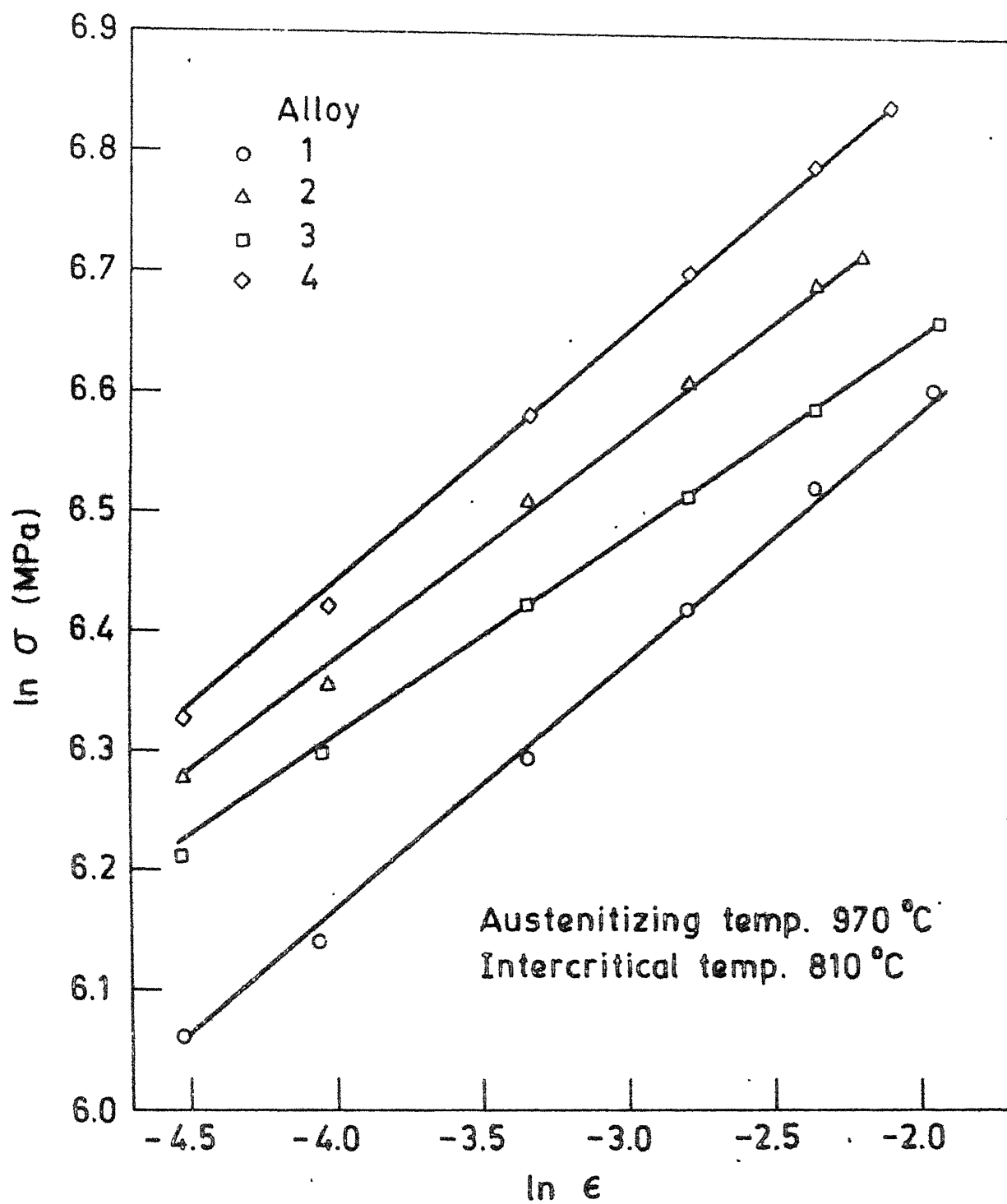
FIG. 4.11. EFFECT OF INTERCRITICAL TEMPERATURE ON TENSILE DUCTILITY.

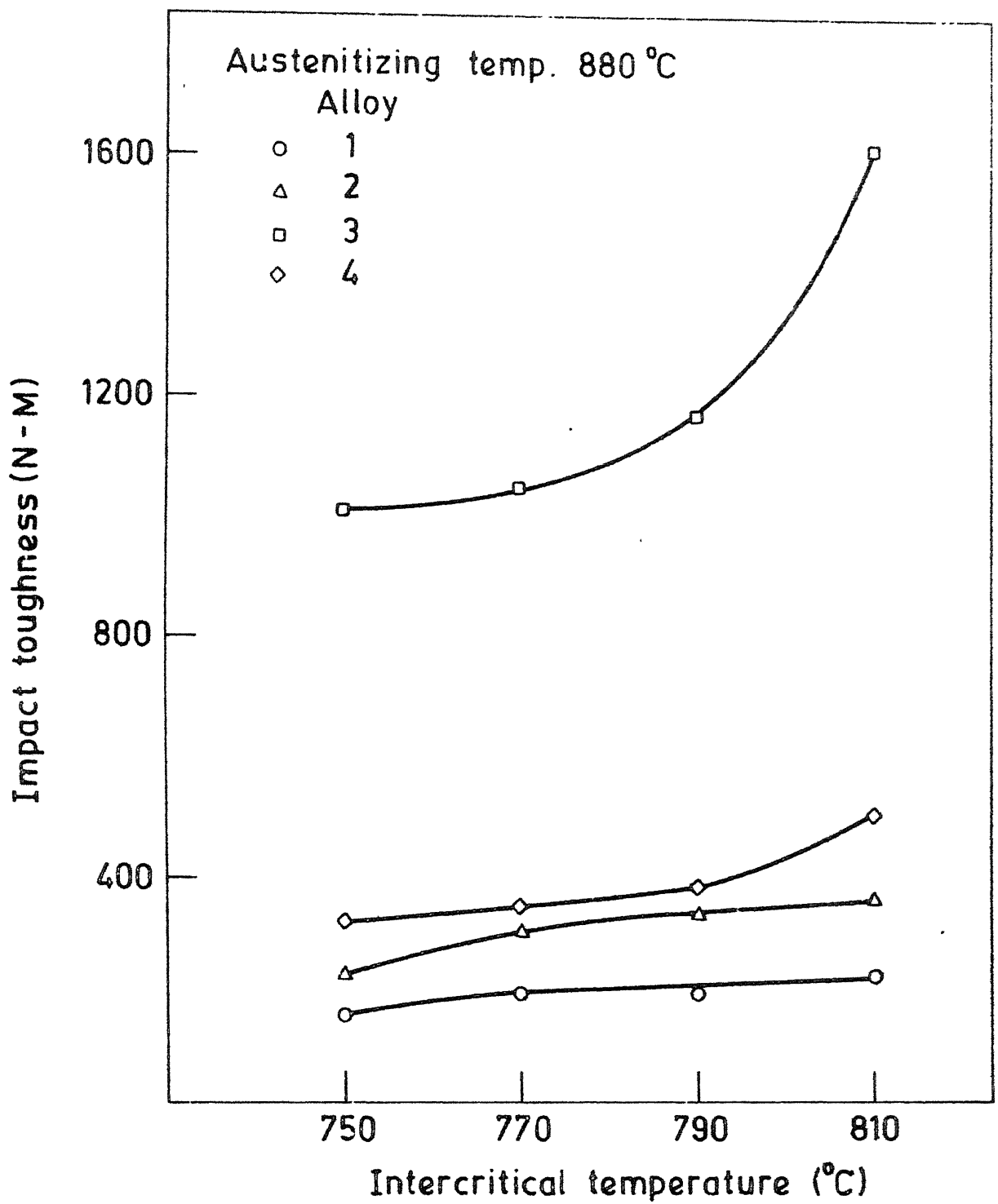FIG. 4.12. PLOT OF ln σ (TRUE-STRESS) vs ln ε (TRUE-STRA

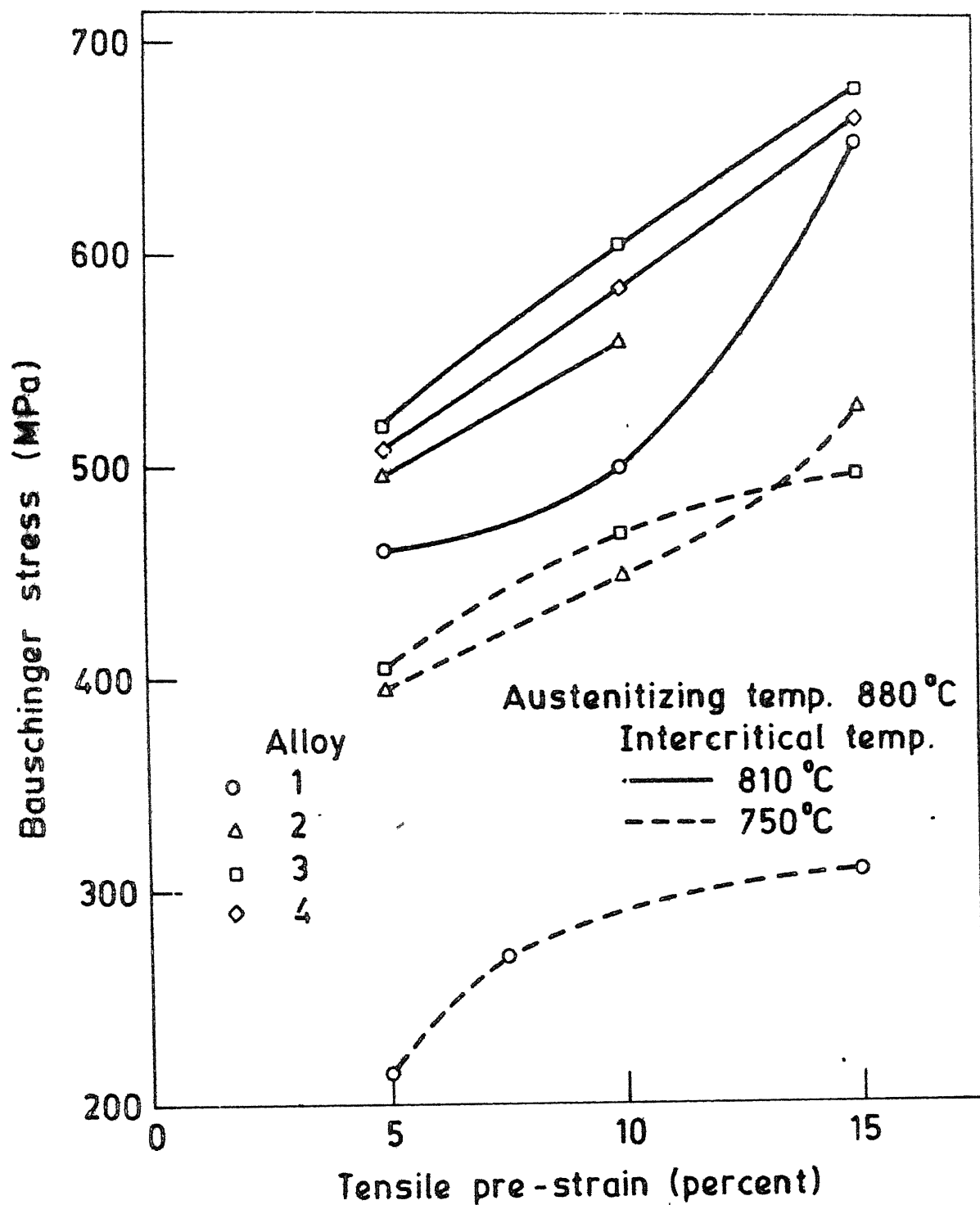FIG. 4.13. EFFECT OF INTERCRITICAL TEMPERATURE ON CHARPY IMPACT TOUGHNESS.

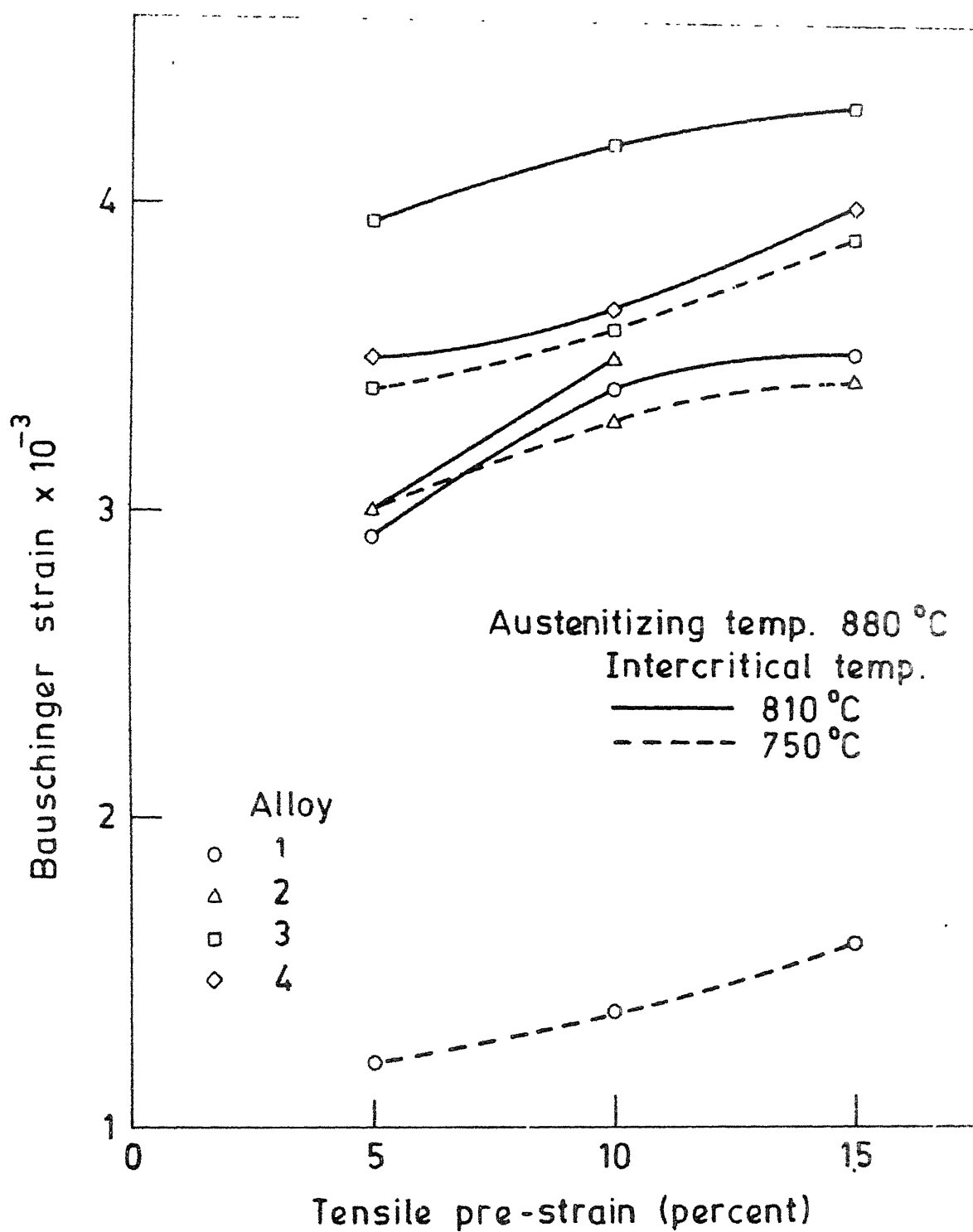FIG. 4.14. EFFECT OF TENSILE PRE-STRAIN ON BAUSCHINGE
STRESS.

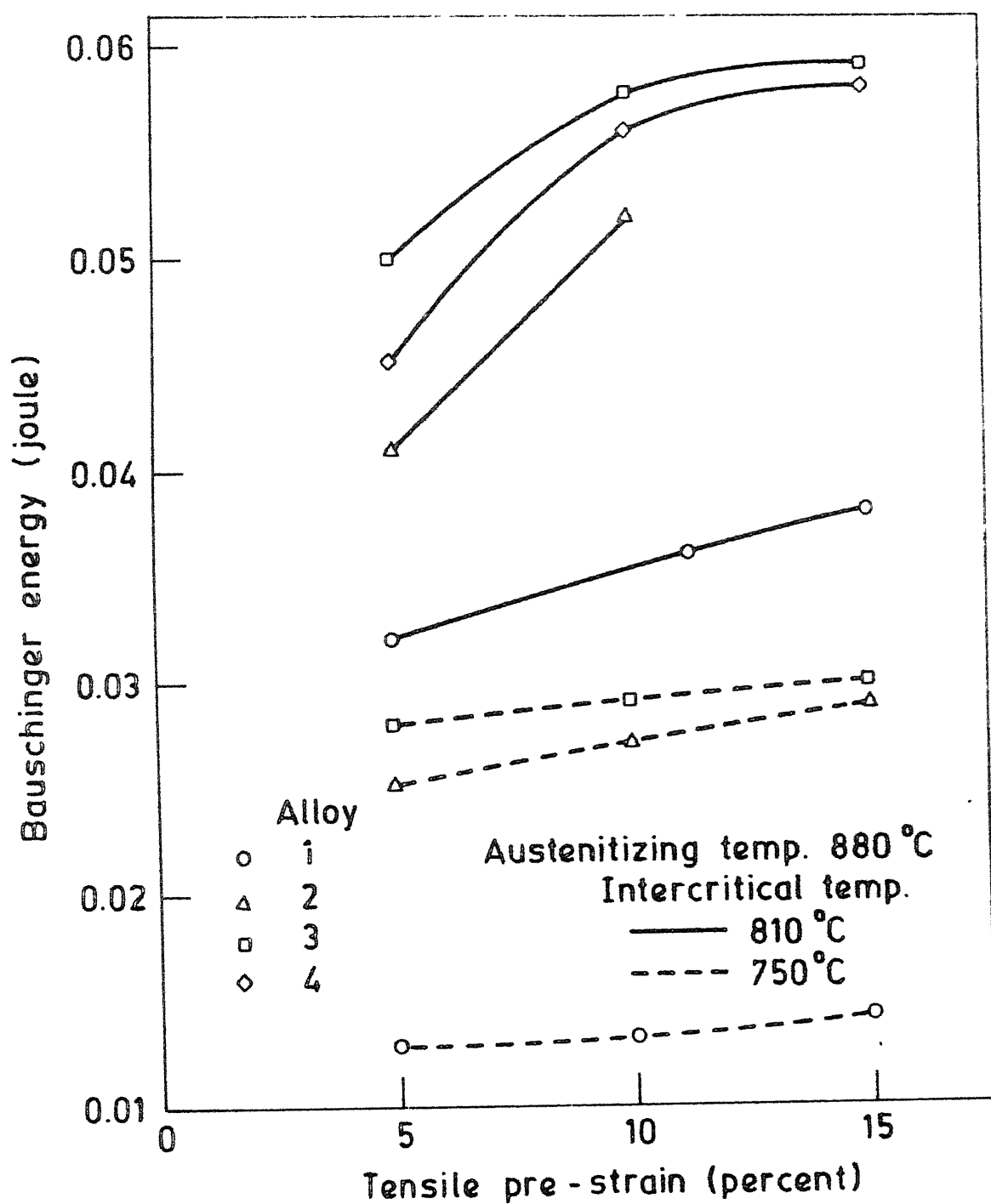FIG. 4.15. EFFECT OF TENSILE PRE-STRAIN ON BAUSCHINGER STRAIN.

FIG. 4.16. EFFECT OF TENSILE PRE-STRAIN ON BAUSCHINGER ENERGY.

CHAPTER V

DISCUSSION

5.1 Microstructural Features:

The existence of globular martensite along grain bound-
aries of ferrite matrix may be attributed to the heterogeneous
nucleation of austenite at pre-existing ferrite grain boundaries
during intercritical annealing.

Further, increase in the martensite content with inter-
critical temperature is due to the fact that the volume fraction
of austenite formed during intercritical annealing would obvi-
ously increase with intercritical temperature. The amount of
martensite formed during a post-anneal quench is an indication
of the amount of austenite which was present at that intercritical
temperature. Higher martensite content in alloys 3 and 4 is due
to presence of higher amount of Mn which increases the harden-
ability of steels. On the other hands, silicon does not have any
significant effect on hardenability. Presence of small amount
of vanadium in each alloy further enhances the hardenability.

Larger grain size at lower intercritical temperatures for
a given austenitizing temperature is probably due to the fact
that a greater degree of ferrite grain coarsening takes place at
a lower intercritical temperature due to a lesser volume fraction
of austenite in comparison to higher intercritical temperature.
Further, the observation that ferrite grains are coarser in
specimens annealed at higher austenitizing temperature for a
given intercritical temperature can be attributed to higher degree

of grain growth taking place at a higher austenitizing temperature in comparison to the lower austenitizing temperature. Vanadium acts as a grain refiner in reducing the grain size in contrast to vanadium free dual phase steels.

5.2 Tensile Properties:

The present observations relating to the yield behavior are similar to the widely reported behavior in the literature. In all these cases, the absence of discontinuous yielding can be attributed to residual stresses and high dislocation density surrounding martensite islands, thus eliminating the yield point as in temper-rolled steels. Ferrite adjacent to martensite is likely to be plastically deformed due to martensitic transformation at relatively low temperatures and thus may contain high density of unpinned dislocations which would lead to gradual yielding at a relatively low stress level.

The increase in the strength values with intercritical temperature in the present study suggests that strength in dual phase steels is determined to a larger extent by the martensite volume fraction. This is in agreement with previous results on dual phase steels. The increase in ultimate tensile strength with decrease in austenitizing temperature is attributed to finer ferrite grains at lower austenitizing temperature. The higher strength in alloy 4 is due to the presence of higher amount of manganese which resulted in more martensite. For a given amount of manganese, increase in silicon content led to slightly more strengthening probably due to solid solution strengthening of the ferrite matrix.

Further, the decrease in ductility with intercritical temperature is due to increase in the amount of hard and brittle phase (martensite) as reported in previous studies. In contrast to the previous studies, the log σ vs. log ε plots were found ɔ be linear over the whole strain range in all alloys of the present study. Thus a single value of work hardening coefficient exists in each case.

5.3 Impact Toughness:

From the test, it can be concluded that soft ferrite phase can be toughened by a fine dispersion of a stronger phase martensite. The improvement of toughness in dual phase steels in comparison to HSLA steels can be attributed to the following factors:

(i) Grain refinement of ferrite phase which is easily attained in dual phase steels.

(ii) Martensite plays an important role in two ways:

   (a) Any crack formed in ferrite is stopped when it reaches a martensite island thereby leading to crack blunting.

   (b) Stress relaxation by plastic flow in tougher martensite phase. It helps in relieving local stresses in the ferrite that would otherwise initiate cracks in ferrite matrix.

The increase in the impact toughness with intercritical temperature is probably due to the combined effect of finer ferrite grains and increased volume fraction of martensite. Difference in the impact toughness of various alloys suggests that silicon decreases the toughness whereas manganese increases

5.4 Bauschinger Effect:

Present study (Figures 4.14, 4.15 and 4.16) indicates that Bauschinger effect in dual phase steels is higher that of usual HSLA steels. This is due to introduction of second hard phase martensite into ferrite matrix.

The increase in the Bauschinger effect with tensile prestrain may be attributed to the fact that there is more and more piling up of dislocations at the obstacles with increasing tensile prestrain due to strain hardening phenomenon thereby leading to a higher back stress.

Bauschinger effect increases with intercritical temperature due to presence of higher amount of martensite. The increased volume fraction of martensite in ferrite matrix makes slip, which originates in ferrite matrix, more difficult. The increase in Bauschinger effect with decreasing austenitizing temperature is due to grain refinement of ferrite at lower austenitizing temperature. The grain boundaries act as additional obstacles for dislocation pile-ups. The higher Bauschinger response in alloys 3 and 4 may be attributed to finer ferrite grains and comparatively more martensite due to higher manganese content.

On assessing the Bauschinger effect in terms of Bauschinger parameters, it is observed that Bauschinger effect changes rapidly in initial stages of prestrain and then it becomes independent of prestrain at later stages.

Thus the observations of tensile, impact and Bauschinger behavior have shown that the properties of dual phase steels are

a function of relative proportions of martensite, ferrite grain size and alloying elements. It is thus possible to develop different combinations of strength, ductility, toughness and Bauschinger response in dual phase steels through the control of composition and heat-treatment parameters.

CHAPTER VII

SUGGESTIONS FOR FUTURE WORK

(1)   A detailed transmission electron microscopy of these steels should be done to explore the substructural details, such as the presence of any retained austenite, carbide precipitation, epitaxial ferrite, type of martensite and dislocation distributions.

(2)   Scanning electron microscopy of fractured surfaces of these steels is needed to ascertain the mode of fracture.

(3)   The effect of other heat-treatment parameters such as cooling rate on the microstructure and mechanical properties can be explored for a better understanding of the overall behavior of these steels. Effect of alloying elements in relation to heat-treatment parameters should be explored with a view to optimize the properties of dual phase steels.

(4)   A mathematical modelling of the composite strengthening due to the combination of a ductile and a hard phase needs to be developed to account for the overall strengthening of the dual phase steels.

REFERENCES

1. Repas P.E., VANITEC'78, VO29 (1978) 18.

2. Davenport A.T., ed., Proceedings of Symposium on "Formable HSLA and Dual Phase Steels", AIME, New York (1977).

3. Proceedings of Seminar on "Dual Phase Steel and Cold Pressing Vanadium Steels in the Automobile Industry", VANITEC'78, West Berlin, VO29 (1978).

4. Kot R.A. and Morris J.W., eds., Proceedings of Symposium on "Structure and Properties of Dual Phase Steels", AIME, New York (1979).

5. Cairns R.L. and Charles J.A., JISI, 205 (1967) 1044.

6. Grange R.A., Proceedings of 2nd International Conference on "Strength of Metals and Alloys", ASM, Metals Park, 3 (1970) 861.

7. Matsuoka T. and Yamamori K., Met. Trans., 6A (1975) 1613.

8. Hayami S. and Furakawa T., Microalloying '75, 2 (1977) 78.

9. Rashid M.S., SAE Preprint, 760206 (1976).

10. Rashid M.S., SAE Preprint, 770211 (1977).

11. Koo J.Y. and Thomas G., Mat. Sci. and Engg., 24 (1976) 187

12. Koo J.Y. and Thomas G., Met. Trans., 8A (1977) 525.

13. Davies R.G., Met. Trans., 9A (1978) 41.

14. Davies R.G., Met. Trans., 9A (1978) 451.

15. Davies R.G., Met. Trans., 9A (1978) 671.

16. Davies R.G., Met. Trans., 10A (1979) 113.

17. Davies R.G., Met. Trans., 10A (1979) 1549.

18. Mileiko S.T., J. Mat. Sci., 4 (1969) 974.

19. Speich G.R. and Miller R.L., "Structure and Properties of Dual Phase Steels", AIME, New York (1979) 145.

20. Tamura I., Tomata Y. and Ozawa H., Proceedings of the 3rd International Conference on "Strength of Metals and Alloys", Cambridge, 1 (1973) 611.

21. Bucher J.H. and Hamburg E.G., "Formable HSLA and Dual Phase Steels", Chicago, AIME (1977) 144.

22. Nakaoka K., Araki K. & Kurihara K., "Formable HSLA and Dual Phase Steels", AIME, New York (1977) 1128.

23. Tanaka T., Nishida M., Hashiguchi K. and Kato T., "Structure and Properties of Dual Phase Steels", AIME, New York (1979) 221.

24. Furukawa T., Morikawa H., Takechi H. and Koyama K., "Structure and Properties of Dual Phase Steels", AIME, New York (1979) 281.

25. Nakaoka K., Hosoya Y., Ohmura M. and Nishimoto A., "Structure and Properties of Dual Phase Steels", AIME, New York (1979) 330.

26. Morrow J.W., Tither G. and Buck R.M., "Formable HSLA and Dual Phase Steels", AIME, New York (1977) 153.

27. Coldren A.P., Tither G., Cornford A. and Miam J.R., "Formable HSLA and Dual Phase Steels", AIME, New York (1977) 205.

28. Eldis G.T., "Structure and Properties of Dual Phase Steels", AIME, New York (1979) 202.

29. Marder A.R. and Bramfitt B.L., "Structure and Properties of Dual Phase Steels", AIME, New York (1979) 242.

30. Marder A.R., "Formable HSLA and Dual Phase Steels", AIME, New York (1977) 89.

31. Rigsbee J.M. and Vander Arend P.J., "Formable HSLA and Dual Phase Steels", AIME, New York (1977) 56.

32. Rigsbee J.M., Abraham J.K. & Devenport A.T., "Structure and Properties of Dual Phase Steels", AIME, New York (1979) 304.

33. Cribbs W.R. and Rigsbee J.M., "Structure and Properties of Dual Phase Steels", AIME, New York (1979) 91.

34. Asmura S., VANITEC '78, VO29 (1978) 43.

35. Coldren A.P. and Tither G., J. Metals, 30 (1978) 6.

36. Kurihara T., Nakaoka K., Yamaguchi, T. and Kuoda H., Iron and Steel Engr., 51 (1974) 39.

37. Thomas G. and Koo J.Y., "Structure and Properties of Dual Phase Steels", AIME, New York (1979) 183.

38. Beiker J. and Hornbogen E., "Structure and Properties of Dual Phase Steels", AIME, New York (1979) 21.

39. Ostrom P. and Lindgren I., Swedish Institute for Metals, Research Report, IM 1308 (1978).

40. Koo J.Y. and Thomas G., Scripta Met., 13 (1979) 1141.

41. Kim N.J. and Thomas G., Met. Trans., 12A (1981) 483.

42. Koo J.Y. and Thomas G., "Formable HSLA and Dual Phase Steels", AIME, New York (1977) 40.

43. Davies R.G. and Magee C.L., VANITEC '78, V029 (1978) 25.

44. Mausi H. and Takechi H., Trans. ISIJ, 16 (1976) 69.

45. Huppi G.S., Matlock D.K. and Krauss G., Scripta Met., 14 (1980) 1239.

46. Sherman A.M., Met. Trans., 6A (1975) 1035.

47. Demeri M.Y., Met. Trans., 12A (1981) 1187.

48. Araki K., Takanda Y. and Nakaoka K., Trans. ISIJ, 17 (1977) 710.

49. Brown L.M. and Stobbs W.M., Phil. Mag., 73 (1971) 1201.

50. Ashby M.F., "Strengthening Methods in Crystals", (A. Kelly and R.B. Nicholson, Eds.), Elsevier Publishing Co. (1971).

51. Ramos L.F., Huppi, G.S., Krauss and Matlock, "Structure and Properties of Dual Phase Steels", TMS-AIME, New York (1979) 62.

52. Ballinger N.K. and Gladman T., Mat. Sci., (1981) 95.

53. Dieter G., "Mechanical Metallurgy', McGraw-Hill Inc. (1976

54. Fischmeister H. and Karlsson B., Z. Metall., 68 (1977) 311

55. Tamura et al., Trans. ISIJ, 13 (1973) 283.

56. Kumakura N., J. of Japan Soc. Mech. Engrs., 70 (1967) 1287

57. Tomota Y. and Kuroki K., Scripta Metallurgica, 14 (1980) 1037.